Figure S1

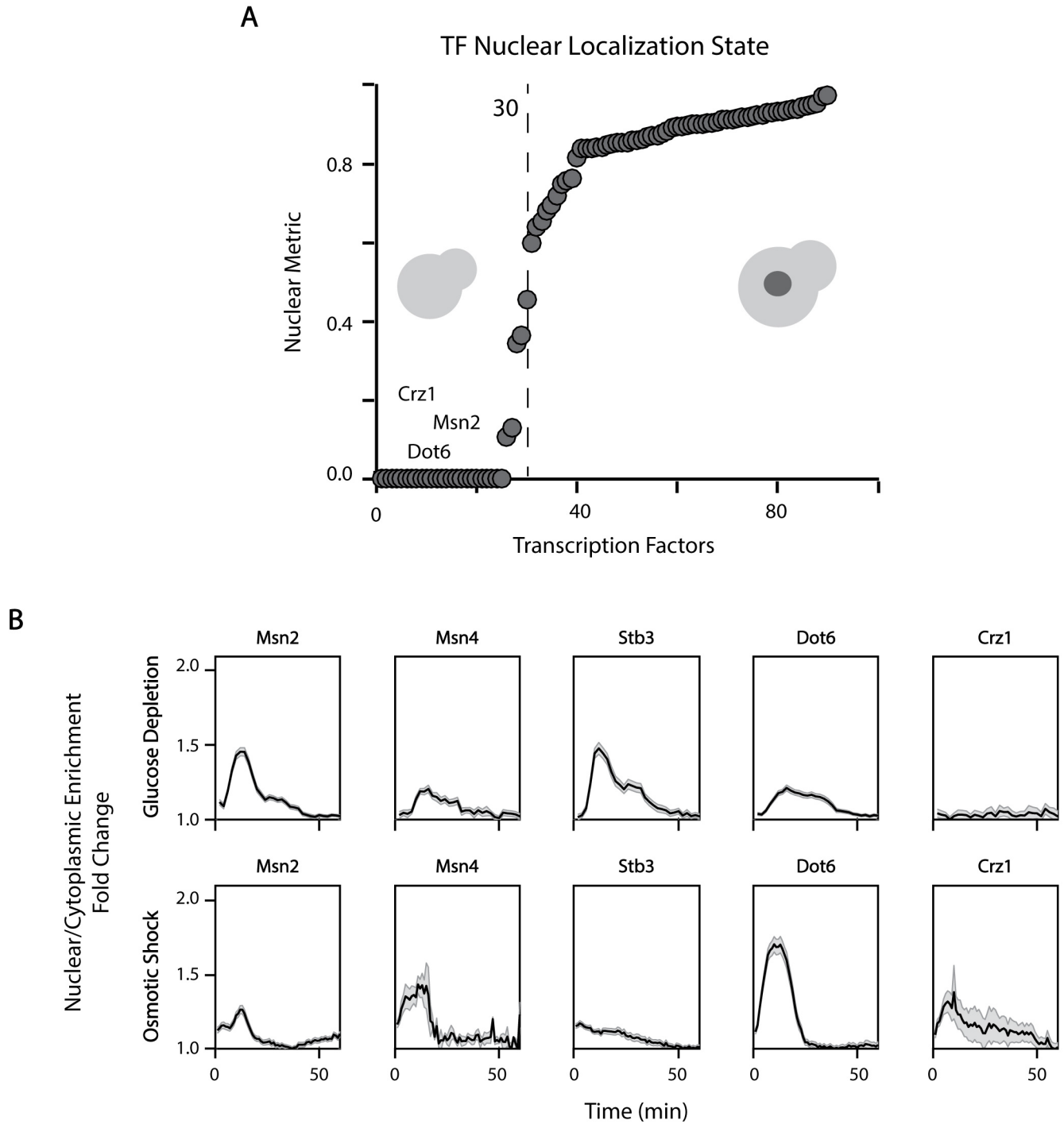
A
TF Nuclear Localization State
30
0.8
0.4
0.0
Nuclear Metric
Crz1
Msn2
Dot6
0
40
80
Transcription Factors
B
Msn2
Msn4
Stb3
Dot6
Crz1
Glucose Depletion
Osmotic Shock
Nuclear/Cytoplasmic Enrichment
Fold Change
2.0
1.5
1.0
0
50
Time (min)

Figure S2

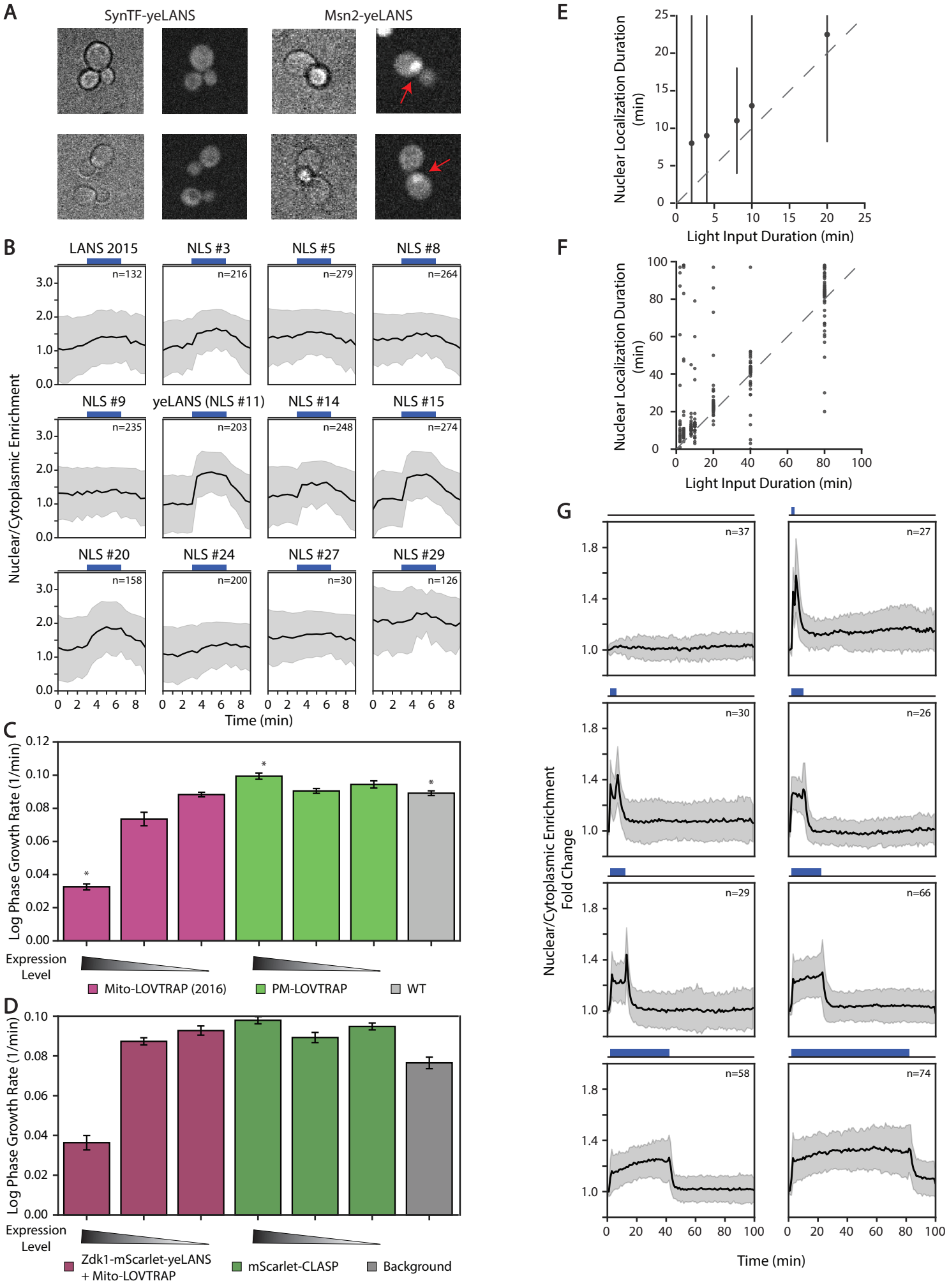
A
SynTF-yeLANS
Msn2-yeLANS
B
LANS 2015
NLS #3
NLS #5
NLS #8
NLS #9
yeLANS (NLS #11)
NLS #14
NLS #15
NLS #20
NLS #24
NLS #27
NLS #29
n=132
n=216
n=279
n=264
n=235
n=203
n=248
n=274
n=158
n=200
n=30
n=126
Nuclear/Cytoplasmic Enrichment
Time (min)
C
Log Phase Growth Rate (1/min)
Expression Level
Mito-LOVTRAP (2016)
PM-LOVTRAP
WT
D
Log Phase Growth Rate (1/min)
Expression Level
Zdk1-mScarlet-yeLANS + Mito-LOVTRAP
mScarlet-CLASP
Background
E
Nuclear Localization Duration (min)
Light Input Duration (min)
F
Nuclear Localization Duration (min)
Light Input Duration (min)
G
n=37
n=27
n=30
n=26
n=29
n=66
n=58
n=74
Nuclear/Cytoplasmic Enrichment Fold Change
Time (min)

Figure S3

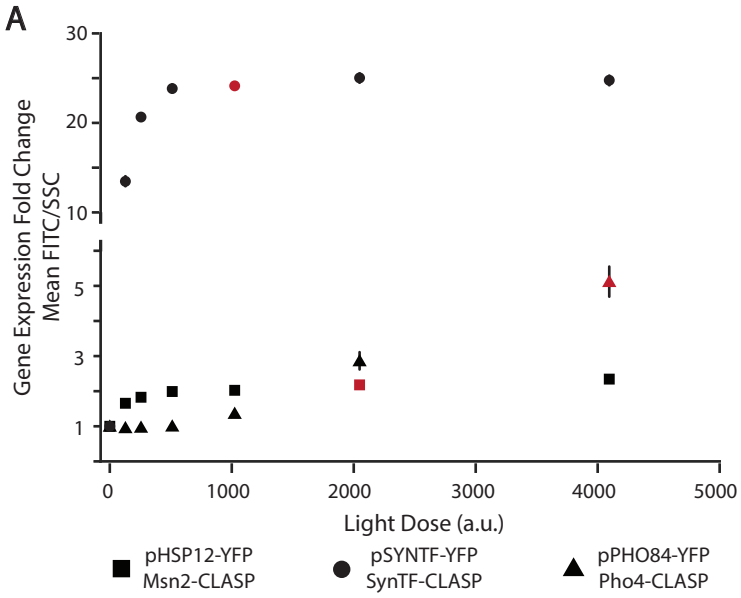
A
Gene Expression Fold Change
Mean FITC/SSC
30
20
10
5
3
1
0
1000
2000
3000
4000
5000
Light Dose (a.u.)
pHSP12-YFP
Msn2-CLASP
pSYNTF-YFP
SynTF-CLASP
pPHO84-YFP
Pho4-CLASP

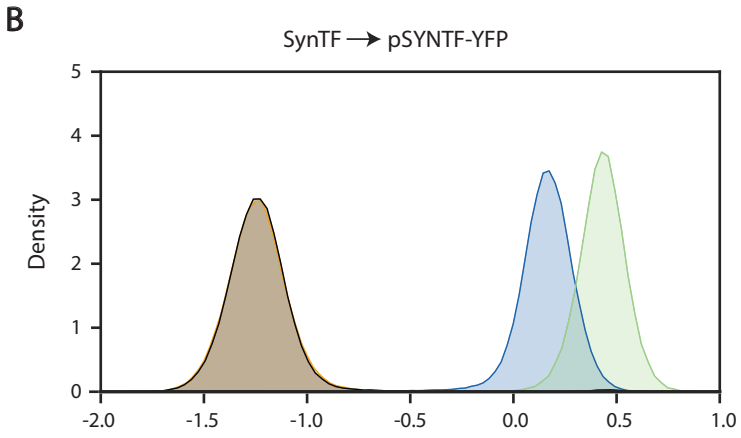
B
SynTF → pSYNTF-YFP
Density
5
4
3
2
1
0
-2.0
-1.5
-1.0
-0.5
0.0
0.5
1.0

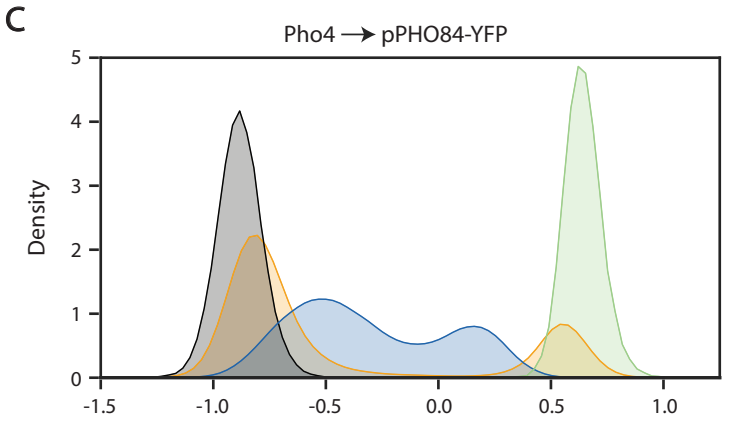
C
Pho4 → pPHO84-YFP
Density
5
4
3
2
1
0
-1.5
-1.0
-0.5
0.0
0.5
1.0

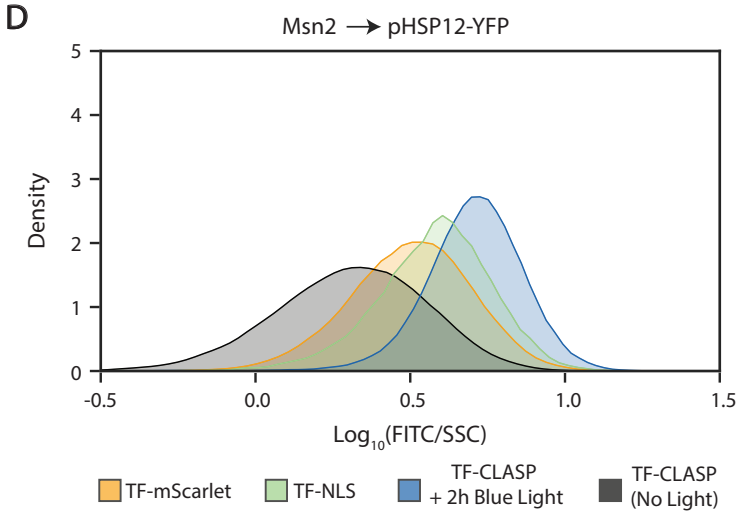
D
Msn2 → pHSP12-YFP
Density
5
4
3
2
1
0
-0.5
0.0
0.5
1.0
1.5
Log10(FITC/SSC)
TF-mScarlet
TF-NLS
TF-CLASP
+ 2h Blue Light
TF-CLASP
(No Light)

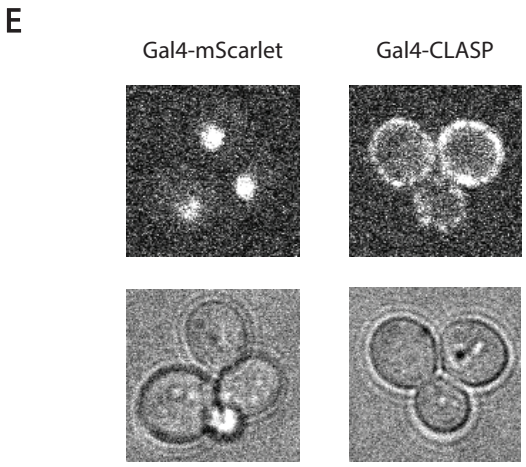
E
Gal4-mScarlet
Gal4-CLASP

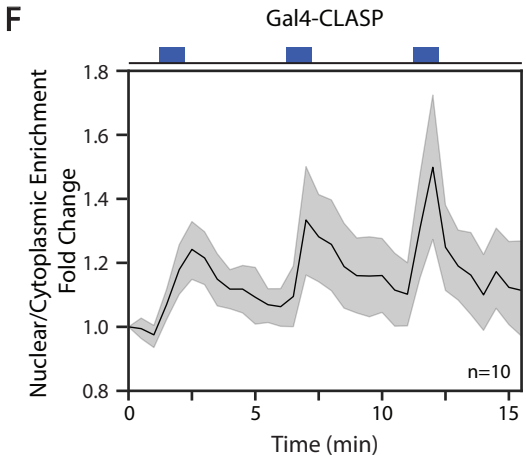
F
Gal4-CLASP
Nuclear/Cytoplasmic Enrichment
Fold Change
1.8
1.6
1.4
1.2
1.0
0.8
n=10
0
5
10
15
Time (min)

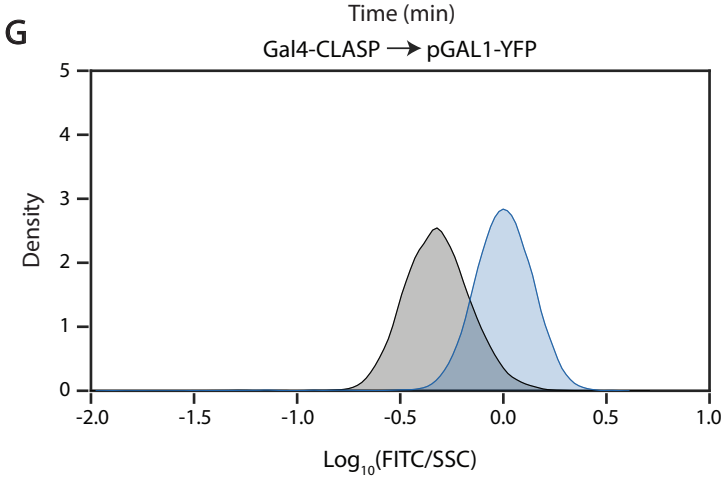
G
Gal4-CLASP → pGAL1-YFP
Density
5
4
3
2
1
0
-2.0
-1.5
-1.0
-0.5
0.0
0.5
1.0
Log10(FITC/SSC)

Figure S4

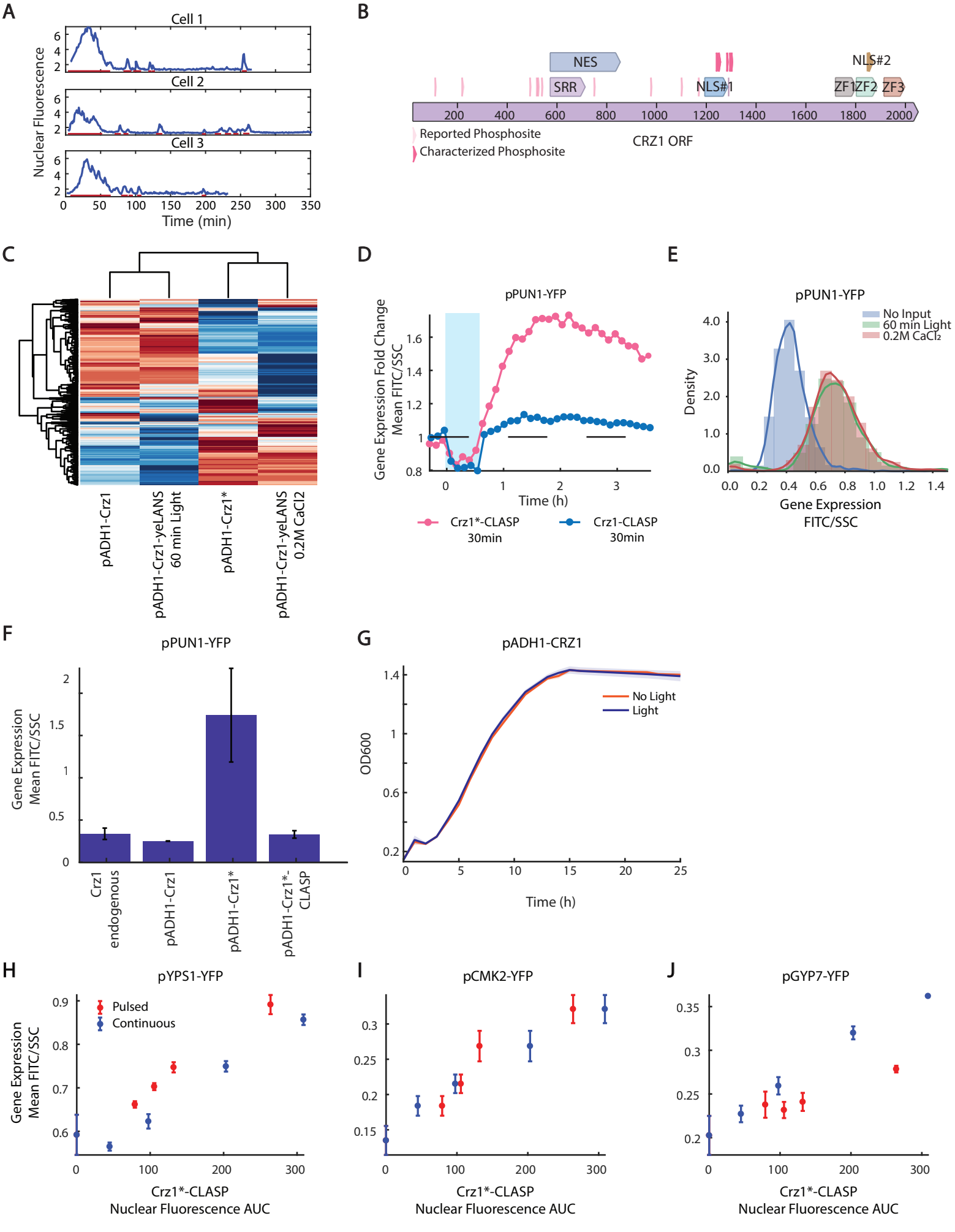
A
Cell 1
Cell 2
Cell 3
Nuclear Fluorescence
Time (min)
B
NES
SRR
NLS#1
NLS#2
ZF1
ZF2
ZF3
Reported Phosphosite
Characterized Phosphosite
CRZ1 ORF
C
pADH1-Crz1
pADH1-Crz1-yeLANS 60 min Light
pADH1-Crz1*
pADH1-Crz1-yeLANS 0.2M CaCl2
D
pPUN1-YFP
Gene Expression Fold Change Mean FITC/SSC
Time (h)
Crz1*-CLASP 30min
Crz1-CLASP 30min
E
pPUN1-YFP
No Input
60 min Light
0.2M CaCl₂
Density
Gene Expression FITC/SSC
F
pPUN1-YFP
Gene Expression Mean FITC/SSC
Crz1 endogenous
pADH1-Crz1
pADH1-Crz1*
pADH1-Crz1*-CLASP
G
pADH1-CRZ1
No Light
Light
OD600
Time (h)
H
pYPS1-YFP
Pulsed
Continuous
Gene Expression Mean FITC/SSC
Crz1*-CLASP Nuclear Fluorescence AUC
I
pCMK2-YFP
Crz1*-CLASP Nuclear Fluorescence AUC
J
pGYP7-YFP
Crz1*-CLASP Nuclear Fluorescence AUC

Figure S5

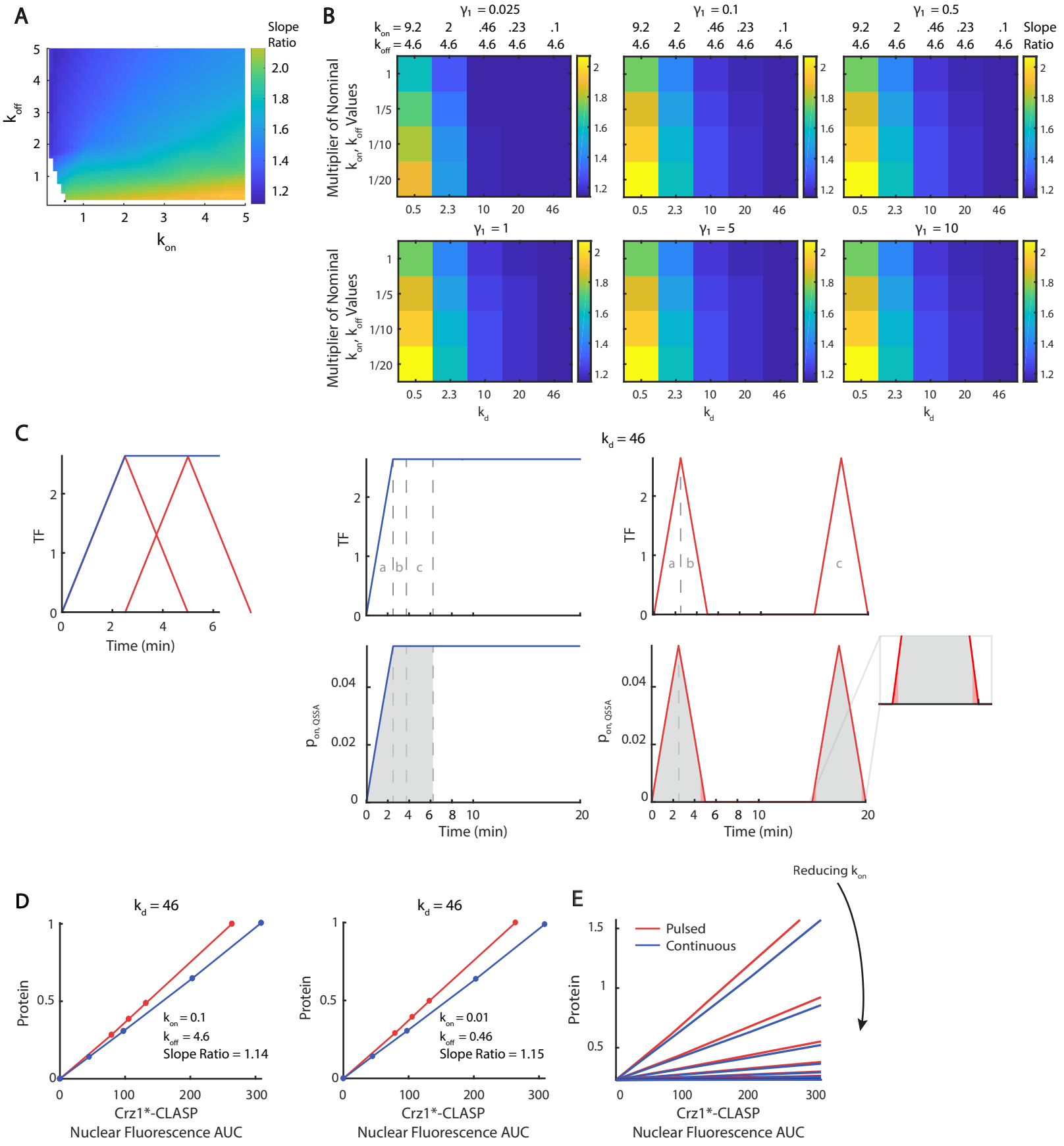
A
Slope Ratio
k_off
k_on
B
γ1 = 0.025
γ1 = 0.1
γ1 = 0.5
γ1 = 1
γ1 = 5
γ1 = 10
k_on = 9.2 2 .46 .23 .1
k_off = 4.6 4.6 4.6 4.6 4.6
Multiplier of Nominal k_on, k_off Values
1 1/5 1/10 1/20
0.5 2.3 10 20 46
k_d
C
TF
Time (min)
k_d = 46
a b c
p_on, QSSA
0.04 0.02 0
0 2 4 6 8 10 20
D
k_d = 46
Protein
k_on = 0.1
k_off = 4.6
Slope Ratio = 1.14
k_on = 0.01
k_off = 0.46
Slope Ratio = 1.15
Crz1*-CLASP
Nuclear Fluorescence AUC
E
Reducing k_on
Pulsed
Continuous

Figure S6

pGYP7-YFP

Dose Response

Cross Validation

A

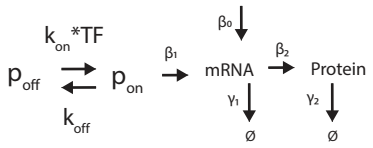

B

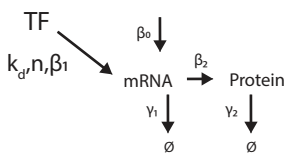

C

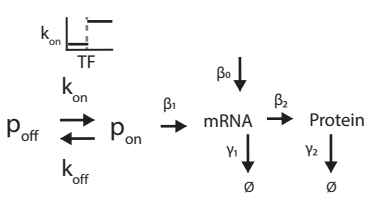

D

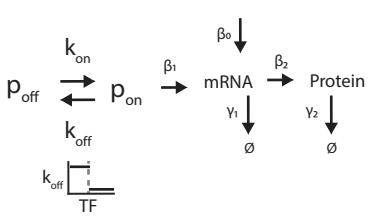

E

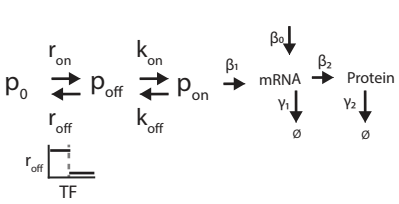

F

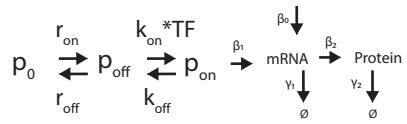

G

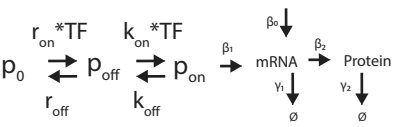

H

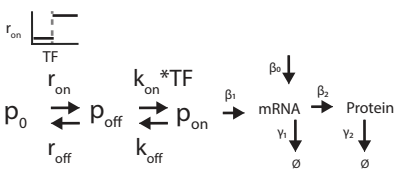

I

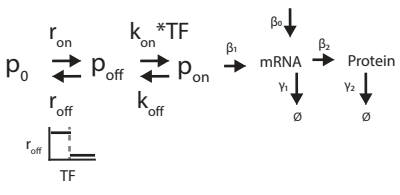

Gene Expression
Mean FITC/SSC

Crz1*-CLASP
Nuclear Fluorescence AUC

Max Crz1*-CLASP
Nuclear Fluorescence

Model

Data

No Light

2m ON/10m OFF

40m ON

• Data

— Model

Figure S7

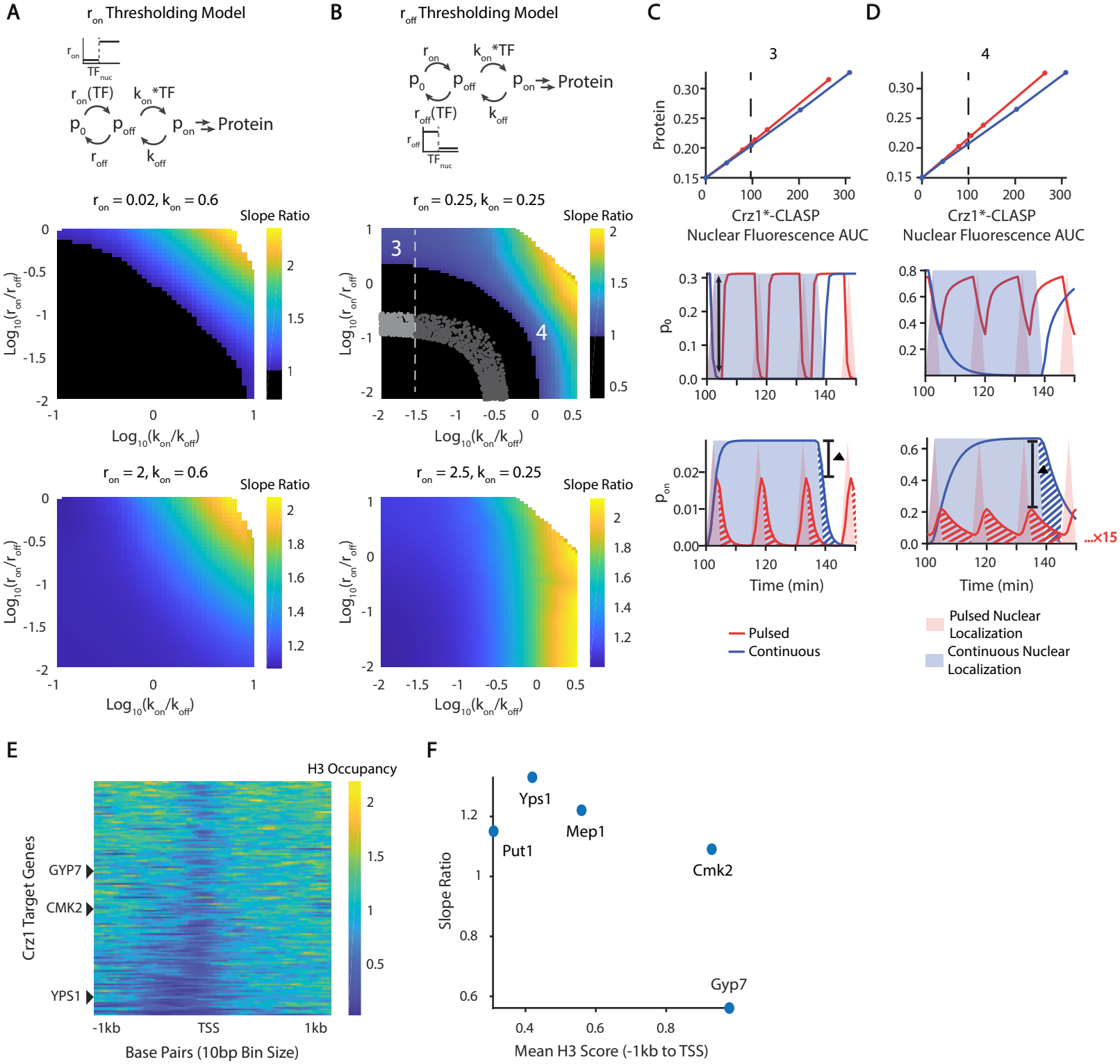
A
r_on Thresholding Model
r_on
TF_nuc
r_on(TF)
k_on*TF
p_0
p_off
p_on
Protein
r_off
k_off
r_on = 0.02, k_on = 0.6
Slope Ratio
Log10(r_on/r_off)
Log10(k_on/k_off)
r_on = 2, k_on = 0.6
B
r_off Thresholding Model
r_off(TF)
r_on = 0.25, k_on = 0.25
r_on = 2.5, k_on = 0.25
3
4
C
D
Protein
Crz1*-CLASP
Nuclear Fluorescence AUC
p_0
p_on
Time (min)
Pulsed
Continuous
Pulsed Nuclear Localization
Continuous Nuclear Localization
...x15
E
H3 Occupancy
Crz1 Target Genes
GYP7
CMK2
YPS1
-1kb
TSS
1kb
Base Pairs (10bp Bin Size)
F
Yps1
Mep1
Put1
Cmk2
Gyp7
Slope Ratio
Mean H3 Score (-1kb to TSS)

Figure S8

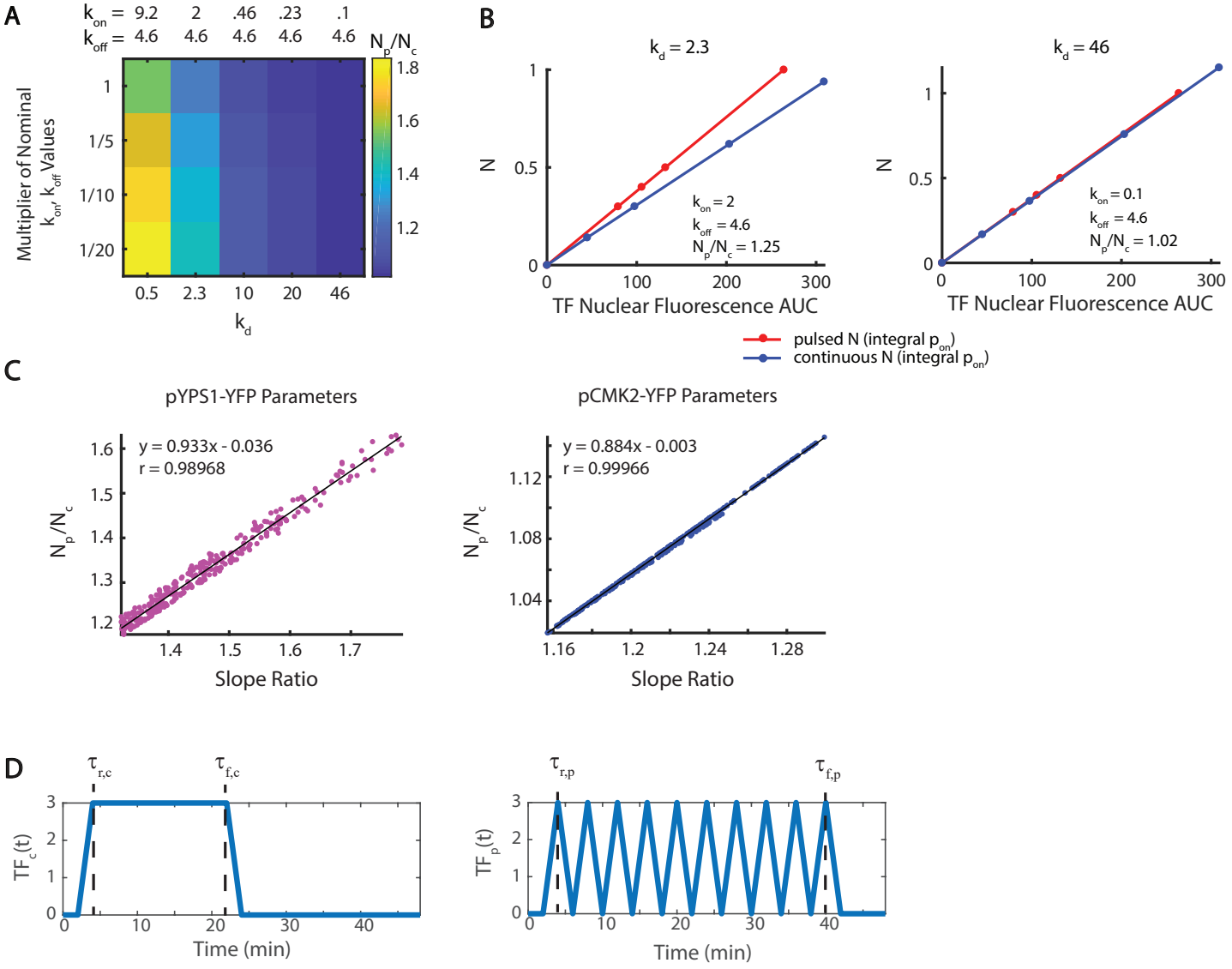
A
k_on = 9.2 2 .46 .23 .1
k_off = 4.6 4.6 4.6 4.6 4.6
N_p/N_c
1.8
1.6
1.4
1.2
Multiplier of Nominal k_on, k_off Values
1
1/5
1/10
1/20
0.5 2.3 10 20 46
k_d
B
k_d = 2.3
k_on = 2
k_off = 4.6
N_p/N_c = 1.25
N
TF Nuclear Fluorescence AUC
k_d = 46
k_on = 0.1
k_off = 4.6
N_p/N_c = 1.02
TF Nuclear Fluorescence AUC
pulsed N (integral p_on)
continuous N (integral p_on)
C
pYPS1-YFP Parameters
y = 0.933x - 0.036
r = 0.98968
N_p/N_c
Slope Ratio
pCMK2-YFP Parameters
y = 0.884x - 0.003
r = 0.99966
N_p/N_c
Slope Ratio
D
τ_r,c
τ_f,c
TF_c(t)
Time (min)
τ_r,p
τ_f,p
TF_p(t)
Time (min)

Figure S9

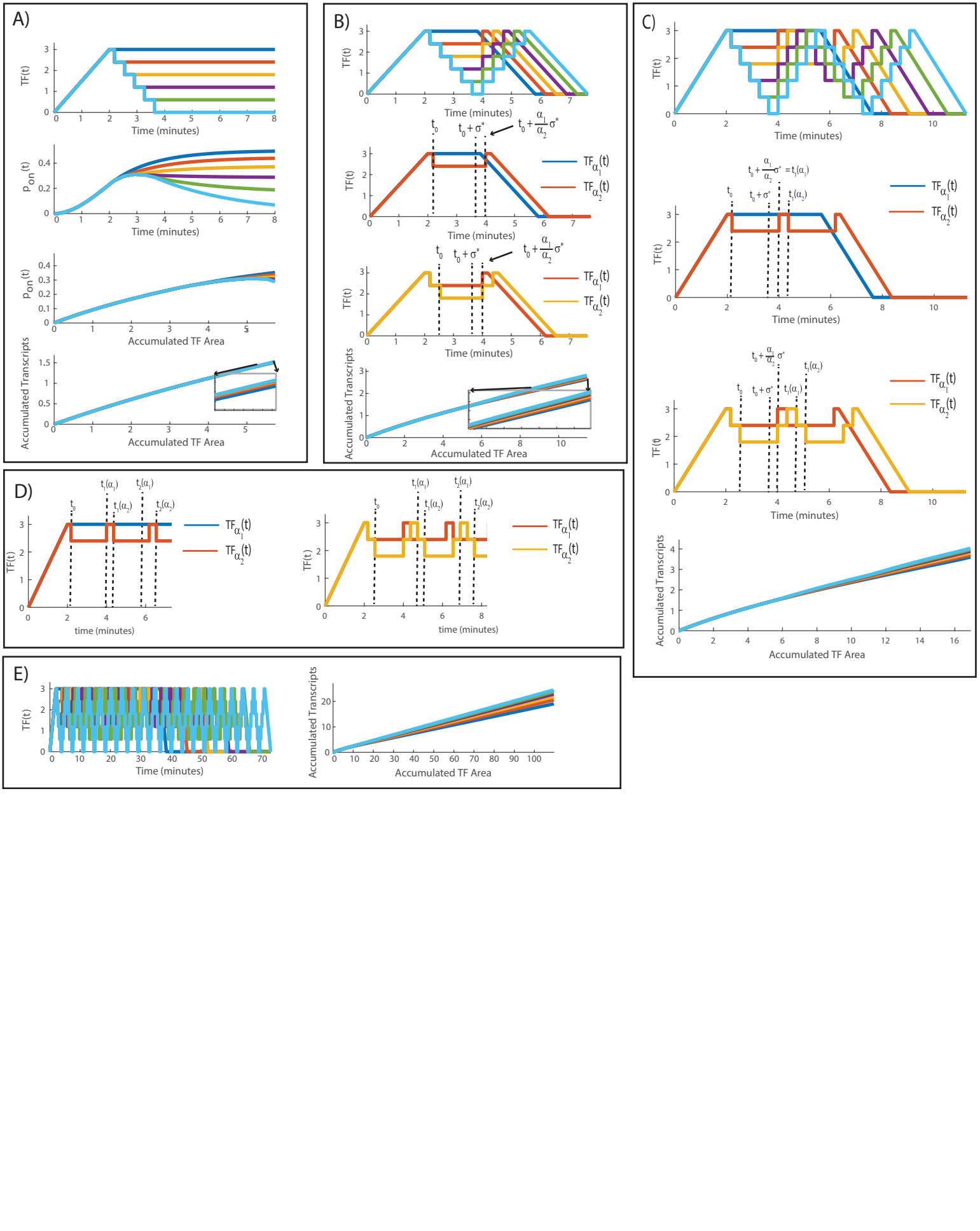
A)
TF(t)
Time (minutes)
p_on(t)
Time (minutes)
p_on(t)
Accumulated TF Area
Accumulated Transcripts
Accumulated TF Area
B)
TF(t)
Time (minutes)
t_0
t_0 + σ*
t_0 + (α_1/α_2)σ*
TF_α1(t)
TF_α2(t)
Time (minutes)
t_0
t_0 + σ*
t_0 + (α_1/α_2)σ*
TF_α1(t)
TF_α2(t)
Time (minutes)
Accumulated Transcripts
Accumulated TF Area
C)
TF(t)
Time (minutes)
t_0 + (α_1/α_2)σ* = t_1(α_1)
t_0
t_0 + σ*
t_1(α_2)
TF_α1(t)
TF_α2(t)
Time (minutes)
t_0 + (α_1/α_2)σ*
t_1(α_2)
t_0
t_0 + σ*
t_1(α_1)
TF_α1(t)
TF_α2(t)
Time (minutes)
Accumulated Transcripts
Accumulated TF Area
D)
t_1(α_1)
t_2(α_1)
t_0
t_1(α_2)
t_2(α_2)
TF_α1(t)
TF_α2(t)
TF(t)
time (minutes)
t_1(α_1)
t_2(α_1)
t_0
t_1(α_2)
t_2(α_2)
TF_α1(t)
TF_α2(t)
TF(t)
time (minutes)
E)
TF(t)
Time (minutes)
Accumulated Transcripts
Accumulated TF Area

Supplementary Figure Captions

Figure S1: Approximately one-third of TFs are basally cytoplasmic in log phase and a subset are shown to exhibit transient nuclear localization, related to Figure 1. A) LOC scores of available transcription factors from the CYCLoPs database are plotted (Chong et al 2015). The LOC score, as defined in Chong et al., 2015, is the number of cells assigned to a specific location (nucleus in this instance) over the total number of cells in any subcellular location. Increasing LOC score denotes increasing nuclear enrichment. **B)** Fold change of nuclear enrichment for a panel of stress-responsive transcription factors (Msn2, Msn4, Stb3, Dot6, and Crz1) are plotted as a function of time in response to environmental inputs (Glucose depletion and osmotic shock). For glucose depletion, SDC media (2% glucose) is replaced with SD media with 0.05% glucose. For osmotic shock, SDC media is replaced with SDC media with 0.95M sorbitol. Imaging begins at t = 0 after addition of environmental perturbation and samples are imaged every 30 seconds. The solid black lines represent the mean of single cell traces and the shading represents the standard error of the mean.

Figure S2: Optimization of LANS and LOVTRAP and CLASP characterization, related to Figure 1. A) Confocal microscopy images of yeast expressing SynTF-yeLANS and Msn2-yeLANS in the absence of blue light. Red arrows (inset) denote examples of cells that exhibit nuclear/cytoplasmic localization of Msn2-yeLANS. **B)** Mean nuclear/cytoplasmic enrichment (nuclear intensity divided by cytoplasm intensity) is plotted as a function of time. Shaded error represents standard deviation and light input regimes are illustrated above graphs. n refers to number of cells tracked and subplot headings (e.g., NLS #3) correspond to NLS peptides listed in Table S1. **C)** Comparison of Mito-LOVTRAP and PM-LOVTRAP strains. Mito-LOVTRAP and PM-LOVTRAP are expressed from pTDH3 (highest), pRPL18B (medium), and pREV1 (lowest) promoters. Strains marked with an asterisk denote those for which growth curves are plotted in Figure 1B of main text. Error bars represent standard error of the linear regression for data from 3 growth experiments. **D)** Comparison of Zdk1-mScarlet-yeLANS + Mito-LOVTrap and CLASP. Both components (e.g. Mito-LOVTRAP and Zdk1-mScarlet-yeLANS) are expressed at the same level, using either pTDH3, pRPL18B, or pREV1 promoters. Background (control strain) denotes the WT strain with pSYNTF-YFP integrated in the LEU locus. Zdk1-mScarlet-yeLANS + Mito-LOVTRAP and mScarlet-CLASP

strains also have this integration. Error bars represent standard error of the linear regression for data from 3 growth experiments. **E)** A zoom-in of Figure 1D in the main text that shows median duration of nuclear localization as a function of light input duration; the line X = Y is denoted by the dashed line. The zoomed graph illustrates that for short pulse durations, the OFF time -- time that nuclear localization extends past the pulse -- is not linearly related to light input duration. **F)** A scatterplot that shows duration of nuclear localization as a function of light input duration. Each point represents a single cell. **G)** Mean nuclear/cytoplasmic enrichment fold change as a function of time for mScarlet-CLASP induced with blue light. Light input regimes are illustrated above graphs (indicating 0, 2, 4, 8, 10, 20, 40, or 80 minute light input). In all plots, except where noted, error (bars or shading) represents standard deviation.

Figure S3: Characterization of TF-CLASP strains, related to Figure 2. A) Mean FITC/SSC is plotted as a function of light intensity (a.u.) for strains that are exposed to different amplitudes of light for two hours (continuous input). Marked in red is the lowest light dose which yielded near-maximal expression for each strain (>90%); this dose is used in all microscopy and flow cytometry experiments for each strain. Error bars represent standard error of the mean for 9 biological replicates. Light doses are quantified in mW in Table S4. **B-D)** Each subplot shows the probability density functions of $\log_{10}$(FITC/SSC) of gene expression of corresponding fluorescent promoter fusion for TF-CLASP, TF-NLS (constitutive nuclear localization), and TF-mScarlet (basal localization) strains. Distributions display expression from 9 biological replicates (data from replicates are pooled). TF-mScarlet strains are not exposed to light, for facile comparison to TF-CLASP (No Light) expression. TF-NLS strains are exposed to two hours of blue light (continuous input) to control for the effect of blue light on YFP fluorescence when comparing to TF-CLASP (Light) expression. For all panels, TF cargos are expressed from pRPL18B. **E)** RFP **(top panels)** and brightfield **(bottom panels)** images of mScarlet-tagged Gal4 **(left panels)** and mScarlet-tagged Gal4-CLASP **(right panels)**. **F)** Gal4 nuclear/cytoplasmic enrichment is plotted as a function of time. Light input regime is illustrated above graph. Shaded gray area represents 95% confidence interval. n refers to the number of cells tracked. **G)** Gene expression of pGal1-YFP resulting from Gal4-CLASP nuclear localization following two hours of blue light input at 25% of the maximal Optoplate intensity. Distributions display expression from 3 biological replicates (data from replicates is pooled). Shown is the probability density function of $\log_{10}$(FITC/SSC) of pGAL1-YFP in the dark (gray) or after light exposure (blue).

Figure S4: Characterization of Crz1, Crz1-CLASP, and Crz1*-CLASP nuclear translocation and gene expression with $CaCl_2$ or blue light input, related to Figure 3. A) Single cell traces of Crz1 nuclear fluorescence over time for 3 representative cells following 0.2M $CaCl_2$. The red lines indicate nuclear localization events. **B)** Schematic of the CRZ1 Open Reading Frame (ORF). Labeled are the Nuclear Localization Sequences (NLS#1 and NLS#2) and the Nuclear Exit Sequence (NES), as well as the Serine-Rich Region (SRR), which is calcium responsive. The light pink triangles denote reported S/T phosphosites, while the dark pink triangles denote reported and characterized S/T phosphosites. The 19 dark and light pink phosphosites are mutated from S/T -> A to construct Crz1*. Phosphosites were identified using PhosphoGRID. **C)** Heatmap of clustered gene expression for 5657 genes. Samples in each column of the heatmap are pADH1-Crz1 with no input, pADH1-Crz1-yeLANS with 60 minutes of light, pADH1-Crz1* with no input, and pADH1-Crz1-yeLANS with 0.2M $CaCl_2$ delivered at the start of the experiment. All samples are in log phase and all measurements are taken 60 minutes after delivery of input. **D)** Gene expression (mean FITC/SSC) of the Crz1 reporter gene pPUN1-YFP driven by either Crz1-CLASP (blue) or Crz1*-CLASP (pink) when given 30 minutes of blue light. Data plotted is for 1 biological replicate. **E)** Probability density functions of gene expression of pPUN1-YFP, measured by FITC/SSC, in response to 0.2M $CaCl_2$ (which causes an initial Crz1 nuclear localization pulse of 40-60 minutes) in a pADH1-Crz1 strain, 60 minutes of blue light exposure in Crz1*-CLASP, and no input in a pADH1-Crz1 strain. Measurements are taken at 4 hours after delivery of input. Data plotted is for 1 biological replicate. **F)** Basal gene expression of pPUN1-YFP for different Crz1 strains: endogenous Crz1, pAdh1-Crz1 in a Crz1 KO background, pAdh1-Crz1* in a Crz1 KO background, and pAdh1-Crz1*-CLASP (without light input) in a Crz1 KO background. Error bars show standard deviation of 3 biological replicates. **G)** OD600, a measurement for growth, plotted as a function of time, for pAdh1-Crz1 with (blue) and without (red) light input (intensity 512 a.u.) over a period of 24 hours, indicating that light exposure does not affect population growth. Measurements are taken every hour. Data plotted is for 3 technical replicates. **H)** Characterization of additional Crz1*-CLASP gene expression in response to blue light, as in Figure 3. Output-Fluorescence plot for pYPS1-YFP. **I)** Output-Fluorescence plot for pCMK2-YFP. **J)** Output-Fluorescence plot for pGYP7-YFP. These data are for 3 biological replicates taken from different days in addition to the data shown in Figure 3. For H-J, error bars are standard deviation of 3 biological replicates.

Figure S5. Higher gene expression of promoters in response to short pulses occurs when the dose response is saturated at low TF concentration, related to Figure 4. A) Heatmap of slope ratio resulting from the model in (Figure 4A) as a function of k_{on} and k_{off}, which both vary from 0.1-5. The ratio k_{off}/k_{on} decreases in a counterclockwise direction on the heatmap. β_1 varies from 0.0001-10, β_0 from 0.000001-0.01 and β_2 from 0.0001-10. The parameter γ_1 is set to 0.06 and γ_2 to 0.0083. **B)** Heatmap of slope ratio for increasing k_d and different values of k_{on} and k_{off}. Each column has a given value of k_d and each row has different values for k_{on} and k_{off} that produce the same k_d. The nominal k_{on} and k_{off} values used in the first row are noted at the top of each column, and every subsequent row uses a fraction of these values (1/5, 1/10, and 1/20). Each heatmap is compiled for a different value of γ_1 shown at the top of each panel. The values of β_1, β_2, and β_0 are 2.01, 4.92, and 0.0032, respectively. **C) (Left panel)** Pulsed and continuous TF inputs, of an equivalent area, used in Figure 4D and S5C are superimposed for comparison of their area. Red and blue lines represent pulsed and continuous inputs, respectively. **(Middle and right panels)** Plot of TF and p_{on} as a function of time for k_d = 46, assuming a fast promoter, therefore generating $p_{on,\ QSSA}$ calculated as $p_{on,\ QSSA} = TF/(TF+ k_d)$. **(Top panels)** Red and blue lines represent pulsed and continuous TF inputs, respectively. Gray lines and text denote equivalent area of TF input. The area labeled “a” represents the rise for both pulsed and continuous inputs. The area labeled “b” represents the fall of the pulsed input, and the equivalent area for the continuous input. The area labeled “c” represents a single pulse of the pulsed input, and the equivalent area of the continuous input. The area labeled “c” is equivalent to the sum of the areas labeled “a” and “b”. The areas labeled “a” and “b” are equivalent to each other. **(Bottom panels)** Red and blue lines represent $p_{on,\ QSSA}$ in response to pulsed and continuous TF inputs, respectively. Gray shading denotes equivalent area of $p_{on,\ QSSA}$ for continuous and pulsed inputs. Light red shading denotes excess $p_{on,\ QSSA}$ area resulting from the rise and fall of the pulsed input. Inset shows the second p_{on} pulse at 200% resolution.**D) (left panel)** Output-Fluorescence plot as in Figure S5D, k_{on} = 0.1 and k_{off} = 4.6. **(right panel)** Output-Fluorescence plot where k_{on} = 0.01 and k_{off} = 0.46. **E)** Output-Fluorescence plot for a parameter set with higher gene expression in response to short pulses. Parameter values are: k_{on} = 1, k_{off} = 0.8, β_1 =0.0001, β_2 = 0.1, γ_1 = 0.05, γ_2 = 0.0083, and β_0 = 0.000001. k_{on} is multiplied by 1/2, 1/4, 1/8, 1/16,and 1/32. The red line represents protein resulting from pulsed inputs and the blue line from continuous inputs.

Figure S6: Exploration of various models for pGYP7-YFP data, related to Figure 6. A) (left panel) Schematic of the kinetic model, where the input is Crz1*-CLASP nuclear localization (TF) and the output is fluorescent protein level (Protein). **(middle left panel)** Output-Fluorescence plot for pGYP7-YFP. Circles are experimentally measured values for at least 3 biological replicates, error bars are standard deviation of those values, while lines denote the output of the model for 200 parameter sets out of 10000 that maximize fits through data points. The solid line denotes the mean and shaded areas the standard deviation of the model outputs. Parameters are sampled (k_{on} from 0.0001-1, k_{off} from 0.0001-1, β_1 from 0.0001-10, β_0 from 0.000001-0.01) or set (β_2 = 0.06, γ_1 = 0.05, γ_2 = 0.0083). **(middle right panel)** Dose response plot for pGYP7-YFP. The parameters that fit the Output-Fluorescence data are used to further fit the dose response of pGYP7-YFP using a best fit to least squared error criterion. Parameter sets below the mean of the least squared error distribution are plotted (solid black line is the mean generated by the model). The black dots are the experimentally measured dose response, and error bars represent standard deviation of at least 3 biological replicates. **(right panel)** The parameters that fit the Output-Fluorescence are then subject to cross-validation using an experiment where Crz1*-CLASP expression is increased (expressed from a pTEF1 promoter), and cells are exposed to either short pulsed (2 minutes ON/10 minutes OFF) or continuous input (40 minutes of light). The model generated outputs (solid red and blue bar) are plotted with the experimental data (hashed red and blue bar). The gray bars are samples not exposed to light. **B) (left panel)** Schematic of a model with cooperativity. **(middle left panel)** Same plots as in (A, middle left panel), with 2481 parameter sets for this model. Parameters are sampled (k_d from 0.01-100, n from 0.5-4, β_1 from 0.0001-10, β_0 from 0.000001-0.01) or set (β_2 = 0.06, γ_1 = 0.05, γ_2 = 0.0083). **(middle right panel, right panel)** Plotted in the same manner as in (A, middle right panel, right panel) with 35 parameter sets. **C) (left panel)** Schematic of a 2-state model with thresholding on the activation constant, k_{on}. **(middle left panel)**. Same plots as in (A, middle left panel), with 148 parameter sets for this model. Parameters are sampled (r_{on} from 0.1-100,r_{off} from 0.1-100, β_1 from 0.0001-10, β_0 from 0.000001-0.01) or set (β_2 = 0.06, γ_1 = 0.05, γ_2 = 0.0083, threshold = 0.5). **(middle right panel, right panel)** Plotted in the same manner as in (A, middle right panel, right panel) with 16 parameter sets. **D) (left panel)** Schematic of a two-state promoter model with a thresholded promoter inactivation constant, k_{off}. **(middle left panel)** Same plots as in (A, middle left panel), with 380 parameter sets for this model. Parameters are sampled (r_{on} from 0.0001-1, r_{off} from 0.0001-1, β_1 from 0.0001-10, β_0 from 0.000001-0.01, threshold from 0-2.7) or set (β_2 = 0.06, γ_1 = 0.05, γ_2 = 0.0083). **(middle right panel, right panel)** Plotted in the same

manner as in (A, middle right panel, right panel) with 52 parameter sets. **E) (left panel)** Schematic of a 3-state model with thresholding in the inactivation constant, r_{off}, between the promoter off-states, p_0 and p_{off}, and no TF dependence in the step before promoter activation. **(middle left panel)** Same plots as in (A, middle left panel), with 423 parameter sets for this model. Parameters are sampled (r_{on} from 0.1-100, r_{off} from 0.1-100, k_{on} from 0.0001-1, k_{off} from 0.0001-1, β_1 from 0.0001-10, β_0 from 0.000001-0.01, threshold from 0-2.7) or set ($\beta_2 = 0.06$, $\gamma_1 = 0.05$, $\gamma_2 = 0.0083$). **(middle right panel, right panel)** Plotted in the same manner as in (A, middle right panel, right panel) with 84 parameter sets. **F) (left panel)** Schematic of a 3-state model with constant rate of transition from p_0 to p_{off}. **(middle left panel)**. Same plots as in (A, middle left panel), with 1288 parameter sets for this model. Parameters are sampled (r_{on} from 0.1-100,r_{off} from 0.1-100, k_{on} from 0.0001-1, k_{off} from 0.0001-1, β_1 from 0.0001-10, β_0 from 0.000001-0.01) or set ($\beta_2 = 0.06$, $\gamma_1 = 0.05$, $\gamma_2 = 0.0083$). **(middle right panel, right panel)** Plotted in the same manner as in (A, middle right panel, right panel) with 16 parameter sets. **G) (left panel)** Schematic of 3-state model with linear dependence on TF in both transitions from p_0 to p_{off} and p_{off} to p_{on}. **(middle left panel)** Same plots as in (A, middle left panel), with 1638 parameter sets for this model. Parameters are sampled (r_{on} from 0.1-100, r_{off} from 0.1-100, k_{on} from 0.0001-1, k_{off} from 0.0001-1, β_1 from 0.0001-10, β_0 from 0.000001-0.01) or set ($\beta_2 = 0.06$, $\gamma_1 = 0.05$, $\gamma_2 = 0.0083$). **(middle right panel, right panel)** Plotted, in the same manner as in (A, middle right panel, right panel) with 228 parameter sets. **H) (left panel)** Schematic of the 3-state model with thresholding in the activation constant, r_{on}, between promoter off-states, p_0 and p_{off}, and linear dependence on TF in transition from p_{off} to p_{on}. **(middle left panel)** Same plots as in (A, middle left panel), with 1649 parameter sets for this model. Parameters are sampled (r_{on} from 0.1-100, r_{off} from 0.1-100, k_{on} from 0.0001-1, k_{off} from 0.0001-1, β_1 from 0.0001-10, β_0 from 0.000001-0.01, threshold from 0-0.5) or set ($\beta_2 = 0.06$, $\gamma_1 = 0.05$, $\gamma_2 = 0.0083$). **(middle right panel, right panel)** Plotted in the same manner as in (A, middle right panel, right panel) with 455 parameter sets. **I) (left panel)** Schematic of the 3-state model with thresholding in the inactivation constant, r_{off}, between promoter off-states, p_0 and p_{off} and linear dependence on TF in transition from p_{off} to p_{on}. **(middle left panel)** Same plots as in (A, middle left panel), with 96 parameter sets for this model. Parameters are sampled (r_{on} from 0.1-100, r_{off} from 0.1-100, k_{on} from 0.0001-1, k_{off} from 0.0001-1, β_1 from 0.0001-10, β_0 from 0.000001-0.01, threshold from 0-0.5) or set ($\beta_2 = 0.06$, $\gamma_1 = 0.05$, $\gamma_2 = 0.0083$). **(middle right panel, right panel)** Plotted in the same manner as in (A, middle right panel, right panel) with 25 parameter sets.

Figure S7: Exploration of the models that fit pGYP7-YFP, related to Figure 6. A) Comparison of the 3-state models with either r_{on} or r_{off} thresholding in the transition from p_0 to p_{off} **(upper panel)** Schematic of the 3-state model with thresholding in the activation rate constant, r_{on}, between promoter off-states p_0 and p_{off}. **(middle panel)** Heatmap of slope ratio in the $\log_{10}(k_{on}/k_{off})$-$\log_{10}(r_{on}/r_{off})$ plane. r_{on} is set to 0.02 and k_{on} = 0.6. Parameters are sampled (r_{off} from 0.0002-0.02, k_{off} from 0.002-0.2) or set (β_1 = 0.0001, β_2 =0.06, γ_1 =0.05, γ_2 =0.0083, threshold= 0.5, β_0 =0.000001). **(lower panel)** Same heatmap as in (A, middle panel) except with r_{on} set to 2, and r_{off} ranges from 0.02-2. **B) (upper panel)** Schematic of the 3-state model with thresholding in the inactivation constant, r_{off}, between promoter OFF-states, p_0 and p_{off}. **(middle panel)** Same heatmap as in (A, middle panel) with r_{on} is set to 0.25 and k_{on} = 0.25, that is previously described in Figure 6E. Parameters are sampled (r_{off} from 0.0025-2.5, k_{off} from 0.0025-0.25) or set (β_1 = 0.0001, β_2 =0.06, γ_1 =0.05, γ_2 =0.0083, threshold= 0.5, β_0 =0.000001). **(lower panel)** Same heatmap as in (B, middle panel) except with r_{on} set to 2.5, and r_{off} ranges from 0.025-25. **C-D)** Additional parameter requirements of the 3-state r_{off} threshold model for fitting pGYP7-YFP. **(upper panels)** Output-Fluorescence plots are generated by the model for different parameter sets that correspond to points 3 and 4 in the heatmap in B. The slope ratio for point 3 is 1.05 with $\log_{10}(k_{on}/k_{off})$ = -1.58 and $\log_{10}(r_{on}/r_{off})$ = 0.6. The slope ratio for point 4 is 1.25 with $\log_{10}(k_{on}/k_{off})$ = 0.1 and $\log_{10}(r_{on}/r_{off})$ = -0.89. Point 3 is chosen to highlight the effect of decreasing r_{off}, while Point 4 is chosen to highlight the effect of decreasing k_{off}. **(middle panels)** Example of a time course of promoter state p_0 for a light input that produces the equivalent of 40 minutes (dotted line in upper panel) in nuclear localization either continuously or in short pulses. Solid lines are the p_0 activity while shading denotes TF nuclear localization. The black double arrow denotes the maximum depletion of the p_0 state for the pulsed input. **(lower panels)** Example of a time course of promoter activity p_{on} for a light input that produces the equivalent of 40 minutes (dotted line in upper panel) in nuclear localization either continuously or in short pulses, similar to the (middle panels). The red and blue hashing represents residual promoter activity beyond the nuclear localization input. The red residual promoter activity is repeated 15 times while the blue residual activity is repeated one time. The ▲ bar denotes the difference between the amplitudes generated by the 2 minute pulsed and 40 minute continuous input. **E)** Correlation of nucleosome occupancy and sensitivity to pulsing. Heatmap of H3 occupancy for the Crz1 target genes as specified by Yoshimoto 2002. H3 occupancy is defined as counts of H3 enrichment over the IgG antibody, which is a control for no pull down of histones. The dataset and determination of start sites are obtained from Sen et al., 2015 and Malabat et al.,

2015, respectively. The software deepTools 2.0 is used to compute the H3 occupancy values. -1 and +1 kb from the transcription start site (TSS) is used. The positions of YPS1, CMK2, and GYP7 in the heatmap are denoted with black triangles. **F)** Slope ratios of Crz1 target genes as a function of their mean H3 nucleosome occupancy scores averaged from -1kb to the Transcription Start Site (TSS). The correlation coefficient is $r^2 = 0.26$.

Figure S8: Slope ratio N_p/N_c of number of transcripts N is strongly correlated with protein slope ratio, related to Figures 4-5 and STAR Methods. A) Heatmap of N_p/N_c for increasing k_d and different values of k_{on} and k_{off}. Each column has a given value of k_d and each row has different values for k_{on} and k_{off} that produce the same k_d. The nominal k_{on} and k_{off} values used in the first row are noted at the top, and every subsequent row uses a fraction of these values (1/5, 1/10, and 1/20). **B)** Plot of N, total transcripts produced, as a function of TF nuclear fluorescence AUC. Left Panel: $k_{on} = 2$, $k_{off} = 4.6$, $k_d = 2.3$ and $N_p/N_c = 1.25$. Right Panel: $k_{on} = 0.1$, $k_{off} = 4.6$, $k_d = 46$ and $N_p/N_c = 1.02$. For both panels, $\beta_1 = 2$, $\gamma_1 = 0.06$, $\beta_2 = 4.92$, $\gamma_2 = 0.0083$, $\beta_0 = 0.0032$. **C)** Plot of slope ratio N_p/N_c of transcripts versus protein slope ratio. N_p are the transcripts produced by $TF_p(t)$ while N_c are those produced by $TF_c(t)$. Each dot represents values computed using the model for a parameter set that fit the protein timecourse and Output-Fluorescence data. Left Panel: data for pYPS1-YFP (also plotted in Figure 5C). Right Panel: Same plot as left panel for pCMK2-YFP (also plotted in Figure 5C). **D)** Time-dependent transcription factor concentration TF(t) for the continuous ($TF_c(t)$, left plot) and pulsed ($TF_p(t)$, right plot) cases. Here $\int TF_c(t)dt = \int TF_p(t)dt$ and both have the same initial rise (shown between 0 and $\tau_{r,c}$ (left graph) and 0 and $\tau_{r,p}$ (right graph)) and final shutoff behavior (shown between $\tau_{f,c}$ and end of input (left graph) and $\tau_{f,p}$ and end of input (right graph)).

Figure S9. Simulations of input sequences that accompany theoretical analysis, related to Figure 4 and STAR Methods. For all simulations I=6 (I is the number of inputs), k_d=3, k_{off} = .33, k_{on} = .11, and $\beta_1 = 1$. **A)** Sequence of inputs used and simulation results for them. (Top panel) Sequence of TF inputs with progressively lower plateaus at successive times. (Top Middle panel) Plots of $p_{on}(t)$ for the different inputs. (Bottom Middle panel) Plots of p_{on} versus. cumulative TF area ($\int_0^t TF(v)\,dv$) for the different inputs. (Bottom plot) Cumulative transcripts ($\beta_1/k_d \int_0^t (1-p_{on}(v))TF(v)dv$) versus cumulative TF area. **B)** Simulation results of cumulative transcripts for a class of inputs that have the same total accumulated TF area. (Top panel) Sequence of TF inputs with progressively lower plateaus at successive times that later rise (step

up) to the level of $TF_c(t)$ shown in dark blue, and then shut off. Light blue line is $TF_p(t)$ with 2 pulses. (Top middle panel) First adjacent input pairs with dark blue being $TF_{\alpha 1}(t)$ and red being $TF_{\alpha 2}(t)$. The plot shows the time of divergence $t=t_0$ for the first two inputs (where $TF_{\alpha 2}(t)$ first drops to its plateau), the time $t=t_0+\alpha_1/\alpha_2\ \sigma^*$ when $TF_{\alpha 2}(t)$ jumps back up to $TF_{\alpha 1}(t)$, and the time $t=t_0+\sigma^*$ where $TF_{\alpha 1}(t)$ has the same corresponding accumulated TF area as $TF_{\alpha 2}(t)$ does at $t=t_0 + \alpha_1/\alpha_2\ \sigma^*$. (Bottom middle panel) Second adjacent input pairs (red is $TF_{\alpha 1}(t)$ and orange is $TF_{\alpha 2}(t)$) with similarly marked time points as in panel above it. (Bottom panel) Cumulative transcripts versus cumulative TF area for the inputs in the top panel. **C)** Extending the class of inputs with equivalent total accumulated TF area from two (panel B) to 3 pulses. (Top panel): Sequence of TF inputs with progressively lower plateaus at successive times that later rise (step up) to the level of $TF_c(t)$ shown in dark blue. Same as in panel B but for 3 pulses. (Top Middle Panel) First adjacent input pairs with dark blue being $TF_{\alpha 1}(t)$ and red being $TF_{\alpha 2}(t)$. There are two additional time labels relative to those in (B). For the $TF_{\alpha 2}(t)$ input, $t=t_1(\alpha_2)$ is the time at which $TF_{\alpha 2}(t)$ drops a second time to its plateau. For the $TF_{\alpha 1}(t)$ input, $t=t_1(\alpha_1)$ is the time at which $TF_{\alpha 1}(t)$ has the same TF area as $TF_{\alpha 2}(t)$ does at $t=t_1(\alpha_2)$. (Bottom middle panel) Second adjacent input pairs (red is $TF_{\alpha 1}(t)$ and orange is $TF_{\alpha 2}(t)$) with similarly marked time points as in panel above it. (Bottom panel): Cumulative transcripts versus cumulative TF(t) area for 3 pulse sequence of inputs shown in top panel. **D)** Extending the class of inputs to M pulses. Plots showing time locations when $TF_{\alpha 2}(t)$ drops to its first, second, and third plateaus for the first adjacent input pair (left plot) and second adjacent input pair (right plot). The times $t=t_0$, $t=t_1(\alpha_2)$ and $t=t_2(\alpha_2)$ are the ordered locations when $TF_{\alpha 2}(t)$ drops to the corresponding plateau. For the $TF_{\alpha 1}(t)$ input, the times $t=t_1(\alpha_1)$ and $t=t_2(\alpha_1)$ map to the same TF area for $TF_{\alpha 1}(t)$ as $t=t_1(\alpha_2)$ and $t=t_2(\alpha_2)$ does for $TF_{\alpha 2}(t)$. **E)** Simulation results for the 20 pulse case. Left plot: All inputs. Dark blue corresponds to the continuous input $TF_c(t)$ of equal area to the other inputs. Light blue corresponds to the pulsed input $TF_p(t)$ (20 pulses). Right plot: Cumulative transcripts versus cumulative TF(t) area.

Supplementary Table Captions

Table S2: List of strains, related to all Figures

Table S3: List of plasmids used to build strains, related to all Figures

Table S4: OptoPlate light intensity characterization, related to Figures 2 and S3

Table S2

Name	Base Strain	Genome	Description	Figure Correspondence	Plasmid
yWCD230	BY4741	BY4741, HIS3 repaired	Wild type strain for plasmid integration	Supp Figure 2C	
yLO213	BY4741	ura3: ConS-pRPL18B-Zdk1-mScarlet-yeLANS-tADH1-Con1-pRPL18B-Hs_RGS2(33-67)_13aa-iRFP713 (iRFP)-asLOV2(404-546)-tPGK1-ConE-URA3 (pSc-native-tSc) leu2: p43_8(8x)-Venus-tPGK1-LEU2 (pSc-native-tSc)	mScarlet-CLASP strain used for microscopy studies (medium expression level)	Figure 1C-E; Supp Figure 2D-G	pLO405, pAN736
yLO133	BY4741	ura3: ConS-pRPL18B-Zdk1-VP16-ZF43_8-mScarlet-yeLANS-tADH1-Con1-pRPL18B-Hs_RGS2(33-67)_13aa-iRFP713 (iRFP)-asLOV2(404-546)-tPGK1-ConE-URA3 (pSc-native-tSc) leu2: p43_8(8x)-Venus-tPGK1-LEU2 (pSc-native-tSc)	SynTF-CLASP	Figure 2; Supp Figure 3A-B	pLO278, pAN736
yLO204	BY4741	leu2: ConLS'-pPHO84-Venus-tPGK1-ConRE'-LEU2 (pSc-native-tSc) ura3: ConS-pRPL18B-Zdk1-Pho4-mScarlet-yeLANS-tADH1-Con1-pTDH3-Hs_RGS2(33-67)_13aa-iRFP713 (iRFP)-asLOV2(404-546)-tPGK1-ConE-URA3 (pSc-native-tSc) PHO4::HIS3	Pho4-CLASP	Figure 2; Supp Figure 3A,C	pLO388, pLO363
yLO228	BY4741	ura3: ConS-pRPL18B-Zdk1-Msn2-mScarlet-yeLANS-tADH1-Con1-pTDH3-Hs_RGS2(33-67)_13aa-iRFP713 (iRFP)-asLOV2(404-546)-tPGK1-ConE'-URA3 (pSc-native-tSc) MSN4::URA3 (broken with 5'FOA) MSN2::HIS3 leu2: ConS-pHsp12-Venus-tPGK1-ConE'-LEU2 (pSc-native-tSc)	Msn2-CLASP	Figure 2; Supp Figure 3A,D	pLO361, pLO352
yLO240	BY4741	ura3: ConLS'-pTDH3-TOM20_TMD(1-39)-iRFP713 (iRFP)-asLOV2(404-546)-tPGK1-ConRE'-URA3 (pSc-native-tSc)	Mito-LOVTRAP (high expression level)	Figure 1B; Supp Figure 2C	pLO485
yLO241	BY4741	ura3: ConLS'-pRPL18B-TOM20_TMD(1-39)-iRFP713 (iRFP)-asLOV2(404-546)-tPGK1-ConRE'-URA3 (pSc-native-tSc)	Mito-LOVTRAP (medium expression level)	Supp Figure 2C	pLO486
yLO242	BY4741	ura3: ConLS'-pREV1-TOM20_TMD(1-39)-iRFP713 (iRFP)-asLOV2(404-546)-tPGK1-ConRE'-URA3 (pSc-native-tSc)	Mito-LOVTRAP (low expression level)	Supp Figure 2C	pLO487
yLO243	BY4741	ura3: ConLS'-pTDH3-Hs_RGS2(33-67)_13aa-iRFP713 (iRFP)-asLOV2(404-546)-tPGK1-ConRE'-URA3 (pSc-native-tSc)	PM-LOVTRAP (high expression level)	Figure 1B; Supp Figure 2C	pLO488
yLO244	BY4741	ura3: ConLS'-pRPL18B-Hs_RGS2(33-67)_13aa-iRFP713 (iRFP)-asLOV2(404-546)-tPGK1-ConRE'-URA3 (pSc-native-tSc)	PM-LOVTRAP (medium expression level)	Supp Figure 2C	pLO489
yLO245	BY4741	ura3: ConLS'-pREV1-Hs_RGS2(33-67)_13aa-iRFP713 (iRFP)-asLOV2(404-546)-tPGK1-ConRE'-URA3 (pSc-native-tSc)	PM-LOVTRAP (low expression level)	Supp Figure 2C	pLO490
yLO210	BY4741	ura3: ConS-pTDH3-Zdk1-mScarlet-yeLANS-tADH1-Con1-pTDH3-Hs_RGS2(33-67)_13aa-iRFP713 (iRFP)-asLOV2(404-546)-tPGK1-ConE-URA3 (pSc-native-tSc) leu2: p43_8(8x)-Venus-tPGK1-LEU2 (pSc-native-tSc)	mScarlet-CLASP (high expression level)	Supp Figure 2D	pLO402, pAN736
yLO215	BY4741	ura3: ConS-pREV1-Zdk1-mScarlet-yeLANS-tADH1-Con1-pREV1-Hs_RGS2(33-67)_13aa-iRFP713 (iRFP)-asLOV2(404-546)-tPGK1-ConE-URA3 (pSc-native-tSc) leu2: p43_8(8x)-Venus-tPGK1-LEU2 (pSc-native-tSc)	mScarlet-CLASP (low expression level)	Supp Figure 2D	pLO407, pAN736
yLO216	BY4741	ura3: ConS-pTDH3-Zdk1-mScarlet-yeLANS-tADH1-Con1-pTDH3-TOM20_TMD(1-39)-iRFP713 (iRFP)-asLOV2(404-546)-tPGK1-ConE-URA3 (pSc-native-tSc) leu2: p43_8(8x)-Venus-tPGK1-LEU2 (pSc-native-tSc)	Zdk1-mScarlet-yeLANS + mito-LOVTRAP (high expression level)	Supp Figure 2D	pLO414, pAN736
yLO219	BY4741	ura3: ConS-pRPL18B-Zdk1-mScarlet-yeLANS-tADH1-Con1-pRPL18B-TOM20_TMD(1-39)-iRFP713 (iRFP)-asLOV2(404-546)-tPGK1-ConE-URA3 (pSc-native-tSc) leu2: p43_8(8x)-Venus-tPGK1-LEU2 (pSc-native-tSc)	Zdk1-mScarlet-yeLANS + mito-LOVTRAP (medium expression level)	Supp Figure 2D	pLO417, pAN736
yLO221	BY4741	ura3: ConS-pREV1-Zdk1-mScarlet-yeLANS-tADH1-Con1-pREV1-TOM20_TMD(1-39)-iRFP713 (iRFP)-asLOV2(404-546)-tPGK1-ConE-URA3 (pSc-native-tSc) leu2: p43_8(8x)-Venus-tPGK1-LEU2 (pSc-native-tSc)	Zdk1-mScarlet-yeLANS + mito-LOVTRAP (low expression level)	Supp Figure 2D	pLO419, pAN736
yLO152	BY4741	ura3: ConS-pRPL18B-VP16-ZF43_8-mScarlet-yeLANS-tADH1-Con1-pRPL18B-Hs_RGS2(33-67)_13aa-iRFP713 (iRFP)-asLOV2(404-546)-tPGK1-ConE-URA3 (pSc-native-tSc) leu2: p43_8(8x)-Venus-tPGK1-LEU2 (pSc-native-tSc)	SynTF-yeLANS	Supp Figure 2A	pLO316, pAN736
yLO179	BY4741	ura3: ConS-pRPL18B-Msn2-mScarlet-yeLANS-tADH1-Con1-pTDH3-Hs_RGS2(33-67)_13aa-iRFP713 (iRFP)-asLOV2(404-546)-tPGK1-ConE'-URA3 (pSc-native-tSc) MSN2::HIS3 leu2: ConS-pHsp12-Venus-tPGK1-ConE'-LEU2 (pSc-native-tSc)	Msn2-yeLANS	Supp Figure 2A	pLO366, pLO352
yLO171	BY4741	ura3: ConS-pRPL18B-VP16-ZF43_8-mScarlet-NLS11-tADH1-Con1-pRPL18B-Hs_RGS2(33-67)_13aa-iRFP713 (iRFP)-asLOV2(404-546)-tPGK1-ConE-URA3 (pSc-native-tSc) leu2: p43_8(8x)-Venus-tPGK1-LEU2 (pSc-native-tSc)	SynTF-NLS11 for comparison to SynTF-CLASP	Supp Figure 3B	pLO344, pAN736
yLO236	BY4741	ura3: ConS-pRPL18B-VP16-ZF43_8-mScarlet-tADH1-Con1-pRPL18B-Hs_RGS2(33-67)_13aa-iRFP713 (iRFP)-asLOV2(404-546)-tPGK1-ConE-URA3 (pSc-native-tSc) leu2: p43_8(8x)-Venus-tPGK1-LEU2 (pSc-native-tSc)	SynTF-mScarlet for comparison to SynTF-CLASP	Supp Figure 3B	pLO411, pAN736
yLO224	BY4741	ura3: ConS-pRPL18B-Pho4-mScarlet-tADH1-Con1-pTDH3-Hs_RGS2(33-67)_13aa-iRFP713 (iRFP)-asLOV2(404-546)-tPGK1-ConE-URA3 (pSc-native-tSc) leu2: ConLS'-pPHO84-Venus-tPGK1-ConRE'-LEU2 (pSc-native-tSc) PHO4::HIS3	Pho4-mScarlet for comparison to Pho4-CLASP	Supp Figure 3C	pLO412, pLO388
yLO225	BY4741	ura3: ConS-pRPL18B-Pho4-mScarlet-NLS11-tADH1-Con1-pTDH3-Hs_RGS2(33-67)_13aa-iRFP713 (iRFP)-asLOV2(404-546)-tPGK1-ConE-URA3 (pSc-native-tSc) leu2: ConLS'-pPHO84-Venus-tPGK1-ConRE'-LEU2 (pSc-native-tSc) PHO4::HIS3	Pho4-NLS11 for comparison to Pho4-CLASP	Supp Figure 3C	pLO465, pLO388

Table S2

yLO229	BY4741	ura3: ConS-pRPL18B-Msn2-mScarlet-NLS11-tADH1-Con1-pTDH3-Hs_RGS2(33-67)_13aa-iRFP713 (iRFP)-asLOV2(404-546)-tPGK1-ConE'-URA3 (pSc-native-tSc) MSN4::URA3 (broken with 5'FOA) MSN2::HIS3 leu2: ConS-pHsp12-Venus-tPGK1-ConE'-LEU2 (pSc-native-tSc)	Msn2-NLS11 for comparison to Msn2-CLASP	Supp Figure 3D	pLO463, pLO352
yLO237	BY4741	ura3: ConS-pRPL18B-Msn2-mScarlet-tADH1-Con1-pTDH3-Hs_RGS2(33-67)_13aa-iRFP713 (iRFP)-asLOV2(404-546)-tPGK1-ConE'-URA3 (pSc-native-tSc) MSN4::URA3 (broken with 5'FOA) MSN2::HIS3 leu2: ConS-pHsp12-Venus-tPGK1-ConE'-LEU2 (pSc-native-tSc)	Msn2-mScarlet for comparison to Msn2-CLASP	Supp Figure 3D	pLO480, pLO352
yLO209	BY4741	ura3: ConS-pRPL18B-Zdk1-Gal4-mScarlet-yeLANS-tADH1-Con1-pTDH3-Hs_RGS2(33-67)_13aa-iRFP713 (iRFP)-asLOV2(404-546)-tPGK1-ConE-URA3 (pSc-native-tSc) leu2: ConS-pGal1-Venus-tPGK1-ConE-LEU2 (pSc-native-tSc) GAL4::HIS5 (JSO His)	Gal4-mScarlet	Supp Figure 3E	pLO413, pAN160
yLO177	BY4741	ura3: ConS-pRPL18B-Zdk1-Gal4-mScarlet-tADH1-Con1-pTDH3-Hs_RGS2(33-67)_13aa-iRFP713 (iRFP)-asLOV2(404-546)-tPGK1-ConE-URA3 (pSc-native-tSc) leu2: ConS-pGal1-Venus-tPGK1-ConE-LEU2 (pSc-native-tSc) GAL4::HIS5 (JSO His)	Gal4-CLASP	Supp Figure 3E-G	pLO364, pAN160
yAHN437	BY4741	leu2: p43_8(8x)-Venus-tPGK1-LEU2 (pSc-native-tSc)	Background strain	Supp Figure 2D	pAN736
ySYC1-78	yBMH35	W303a TPK1/2/3-AS Nhp6a-iRFP (Kan) trp1::pAdh1-mCherry-PEF-NESLOVNLS IRFP-nuclear	Original Yumerefendi LANS construct	Supp Figure 2B	pSYC084
ySYC1-79	yBMH35	W303a TPK1/2/3-AS Nhp6a-iRFP (Kan) trp1::pAdh1-mCherry-PEF-NESLOVNLSvar#3 IRFP-nuclear	class 2 raaKRpRtt	Supp Figure 2B	pSYC085
ySYC1-80	yBMH35	W303a TPK1/2/3-AS Nhp6a-iRFP (Kan) trp1::pAdh1-mCherry-PEF-NESLOVNLSvar#5 IRFP-nuclear	class 2 paaKRpRtt	Supp Figure 2B	pSYC087
ySYC1-81	yBMH35	W303a TPK1/2/3-AS Nhp6a-iRFP (Kan) trp1::pAdh1-mCherry-PEF-NESLOVNLSvar#8 IRFP-nuclear	class 2 apaKRaRtt	Supp Figure 2B	pSYC088
ySYC2-1	yBMH35	W303a TPK1/2/3-AS Nhp6a-iRFP (Kan) trp1::pAdh1-mCherry-PEF-NESLOVNLSvar#11 IRFP-nuclear	class 3 aaaKRswsmaf	Figure 1B; Supp Figure 2B	pSYC090
ySYC2-2	yBMH35	W303a TPK1/2/3-AS Nhp6a-iRFP (Kan) trp1::pAdh1-mCherry-PEF-NESLOVNLSvar#14 IRFP-nuclear	class 3 aaaKRswvmaf	Supp Figure 2B	pSYC091
ySYC2-3	yBMH35	W303a TPK1/2/3-AS Nhp6a-iRFP (Kan) trp1::pAdh1-mCherry-PEF-NESLOVNLSvar#15 IRFP-nuclear	class 3 aaaKRswsaaf	Supp Figure 2B	pSYC092
ySYC2-4	yBMH35	W303a TPK1/2/3-AS Nhp6a-iRFP (Kan) trp1::pAdh1-mCherry-PEF-NESLOVNLSvar#20 IRFP-nuclear	bipartite KRpatlandspaaKRR	Supp Figure 2B	pSYC093
ySYC2-5	yBMH35	W303a TPK1/2/3-AS Nhp6a-iRFP (Kan) trp1::pAdh1-mCherry-PEF-NESLOVNLSvar#4 IRFP-nuclear	class 2 raaKRlRtt	Supp Figure 2B	pSYC086
ySYC2-6	yBMH35	W303a TPK1/2/3-AS Nhp6a-iRFP (Kan) trp1::pAdh1-mCherry-PEF-NESLOVNLSvar#9 IRFP-nuclear	class 2 paaKRlCtt	Supp Figure 2B	pSYC089
ySYC2-7	yBMH35	W303a TPK1/2/3-AS Nhp6a-iRFP (Kan) trp1::pAdh1-mCherry-PEF-NESLOVNLSvar#24 IRFP-nuclear	class 1 KRKRwendip	Supp Figure 2B	pSYC094
ySYC2-8	yBMH35	W303a TPK1/2/3-AS Nhp6a-iRFP (Kan) trp1::pAdh1-mCherry-PEF-NESLOVNLSvar#27 IRFP-nuclear	class 1 psRKRKRdhyav	Supp Figure 2B	pSYC095
ySYC2-9	yBMH35	W303a TPK1/2/3-AS Nhp6a-iRFP (Kan) trp1::pAdh1-mCherry-PEF-NESLOVNLSvar#29 IRFP-nuclear	class 1 tspsRKRKwdqv	Supp Figure 2B	pSYC096
ySYC1-62	yBMH35	W303a TPK1/2/3-AS Nhp6a-iRFP (Kan) trp1::pAdh1-Dot6-mCherry (TRP1) IRFP-nuclear	stress-induced localization experiments for Dot6	Supp Figure 1B	pJSO529
ySYC1-70	yBMH35	W303a TPK1/2/3-AS Nhp6a-iRFP (Kan) trp1::pAdh1-Crz1-mCherry (TRP1) IRFP-nuclear	stress-induced localization experiments for Crz1	Supp Figure 1B	pJSO568
ySYC1-71	yBMH35	W303a TPK1/2/3-AS Nhp6a-iRFP (Kan) trp1::pAdh1-Stb3-mCherry (TRP1) IRFP-nuclear	stress-induced localization experiments for Stb3	Supp Figure 1B	pJSO269
ySYC1-72	yBMH35	W303a TPK1/2/3-AS Nhp6a-iRFP (Kan) trp1::pAdh1-Msn2-mCherry (TRP1) IRFP-nuclear	stress-induced localization experiments for Msn2	Supp Figure 1B	pJSO392
ySYC1-74	yBMH35	W303a TPK1/2/3-AS Nhp6a-iRFP (Kan) trp1::pAdh1-Msn4-mCherry (TRP1) IRFP-nuclear	stress-induced localization experiments for Msn4	Supp Figure 1B	pJSO285
ySYC1-76	yBMH35	W303a TPK1/2/3-AS Nhp6a-iRFP (Kan) trp1::pAdh1-Pho4-mCherry (TRP1) IRFP-nuclear	stress-induced localization experiments for Pho4	Supp Figure 1B	pJSO569
ySYC5-36	ySYC5-26	w303a nhp6a::nhp6a-iRFP(KAN) crz1::sfGFP-CandHIS ura::pADH1-zdk-CRZ1(ALA)-mCherry-yeLANS;pTDH3-Hs_RGS2(33-67)_13aa-iRFP713 (iRFP)-asLOV2(404-546)(URA) leu::pYps1-Venus(LEU)	promoter fusions driven by Crz1*-CLASP; pYps1-YFP	Figure 3-5; Supp Figure 4H	pSYC332
ySYC5-37	ySYC5-26	w303a nhp6a::nhp6a-iRFP(KAN) crz1::sfGFP-CandHIS ura::pADH1-zdk-CRZ1(ALA)-mCherry-yeLANS;pTDH3-Hs_RGS2(33-67)_13aa-iRFP713 (iRFP)-asLOV2(404-546)(URA) leu::pGyp7-Venus(LEU)	promoter fusions driven by Crz1*-CLASP; pGyp7-YFP	Figure 3, 6; Supp Figure 4J, 6	pSYC392
ySYC5-38	ySYC5-26	w303a nhp6a::nhp6a-iRFP(KAN) crz1::sfGFP-CandHIS ura::pADH1-zdk-CRZ1(ALA)-mCherry-yeLANS;pTDH3-Hs_RGS2(33-67)_13aa-iRFP713 (iRFP)-asLOV2(404-546)(URA) leu::pPut1-Venus(LEU)	promoter fusions driven by Crz1*-CLASP; pPut1-YFP	Figure 3C	pSYC393
ySYC5-40	ySYC5-26	w303a nhp6a::nhp6a-iRFP(KAN) crz1::sfGFP-CandHIS ura::pADH1-zdk-CRZ1(ALA)-mCherry-yeLANS;pTDH3-Hs_RGS2(33-67)_13aa-iRFP713 (iRFP)-asLOV2(404-546)(URA) leu::pCmk2-Venus(LEU)	promoter fusions driven by Crz1*-CLASP; pCmk2-YFP	Figure 3-5; Supp Figure 4I	pSYC395
ySYC5-43	ySYC5-26	w303a nhp6a::nhp6a-iRFP(KAN) crz1::sfGFP-CandHIS ura::pADH1-zdk-CRZ1(ALA)-mCherry-yeLANS;pTDH3-Hs_RGS2(33-67)_13aa-iRFP713 (iRFP)-asLOV2(404-546)(URA) leu::pEna1-Venus(LEU)	promoter fusions driven by Crz1*-CLASP; pEna1-YFP	Figure 3C	pSYC398
ySYC5-45	ySYC5-26	w303a nhp6a::nhp6a-iRFP(KAN) crz1::sfGFP-CandHIS ura::pADH1-zdk-CRZ1(ALA)-mCherry-yeLANS;pTDH3-Hs_RGS2(33-67)_13aa-iRFP713 (iRFP)-asLOV2(404-546)(URA) leu::pMep1-Venus(LEU)	promoter fusions driven by Crz1*-CLASP; pMep1-YFP	Figure 3C	pSYC400
ySYC5-34	ySYC5-26	w303a nhp6a::nhp6a-iRFP(KAN) crz1::sfGFP-CandHIS ura::pADH1-zdk-CRZ1(ALA)-mCherry-yeLANS;pTDH3-Hs_RGS2(33-67)_13aa-iRFP713 (iRFP)-asLOV2(404-546)(URA) leu::pPun1-Venus(LEU)	promoter fusion driven by Crz1*-CLASP; pPun1-YFP	Supp Figure 4E, 4D-F	pSYC331
ySYC5-27	ySYC5-11	w303a nhp6a::nhp6a-iRFP(KAN) crz1::sfGFP-CandHIS ura::pADH1-CRZ(WT)-mCherry(URA) leu::pPun1-Venus(LEU)	Crz1 WT for CaCl2 experiment; flow; rnaseq	Supp Figure 4E, F	pSYC331
ySYC5-32	ySYC5-24	w303a nhp6a::nhp6a-iRFP(KAN) crz1::sfGFP-CandHIS ura::pADH1-zdk-CRZ1(WT)-mCherry-yeLANS;pTDH3-Hs_RGS2(33-67)_13aa-iRFP713 (iRFP)-asLOV2(404-546)(URA) leu::pPun1-Venus(LEU)	promoter fusion driven by Crz1-CLASP; pPun1	Supp Figure 4D	pSYC331
ySYC5-30	ySYC5-13	w303a nhp6a::nhp6a-iRFP(KAN) crz1::sfGFP-CandHIS ura::pADH1-CRZ1(ALA)-mCherry(URA) leu::pPun1-Venus(LEU)	untrapped Crz1*; pPun1; flow; rnaseq	Supp Figure 4C, F	pSYC331
ySYC5-71	ySYC5-69	w303a nhp6a::nhp6a-iRFP(KAN) crz1::sfGFP-CandHIS ura::pADH1-zdk-CRZ1(5A)-mCherry-yeLANS;pTDH3-Hs_RGS2(33-67)_13aa-iRFP713 (iRFP)-asLOV2(404-546)(URA) leu::pPun1-Venus(LEU)	crz1(5A); testing equivalence of crz1* and crz1(5A)	Supp Figure 11	pSYC331
ySYC6-23	ySYC6-7	w303a nhp6a::nhp6a-iRFP(KAN) crz1::sfGFP-CandHIS ura::pTef1-zdk-CRZ(ALA)-mCherry-yeLANS; pTDH3-Hs_RGS2(33-67)_13aa-iRFP713 (iRFP)-asLOV2(404-546) (URA) leu::pGyp7-venus(LEU)	pGYP7-YFP dose response strains (high expression level)	Figure 6C-D, Supp Figure 6	pSYC392
ySYC6-24	ySYC6-6	w303a nhp6a::nhp6a-iRFP(KAN) crz1::sfGFP-CandHIS ura::pRpl18b-zdk-CRZ(ALA)-mCherry-yeLANS; pTDH3-Hs_RGS2(33-67)_13aa-iRFP713 (iRFP)-asLOV2(404-546)(URA) leu::pGyp7-venus(LEU)	pGYP7-YFP dose response strains (low expression level)	Figure 6C, Supp Figure 6	pSYC392
ySYC6-11	ySYC4-34	w303a nhp6a::nhp6a-iRFP(KAN) crz1::sfGFP-CandHIS leu::pGyp7-venus(LEU) P2	pGYP7-YFP dose response strains (Crz1 KO)	Figure 6C, Supp Figure 6	pSYC392
ySYC6-18	ySYC6-7	w303a nhp6a::nhp6a-iRFP(KAN) crz1::sfGFP-CandHIS ura::pTef1-zdk-CRZ(ALA)-mCherry-yeLANS; pTDH3-Hs_RGS2(33-67)_13aa-iRFP713 (iRFP)-asLOV2(404-546)(URA) leu::pYps1-venus(LEU)	pYPS1-YFP dose response strains (high expression level)	Figure 4I	pSYC332

Table S2

ySYC6-19	ySYC6-6	w303a nhp6a::nhp6a-iRFP(KAN) crz1::sfGFP-CandHIS ura::pRpl18b-zdk-CRZ(ALA)-mCherry-yeLANS; pTDH3-Hs_RGS2(33-67)_13aa-iRFP713 (iRFP)-asLOV2(404-546)(URA) leu::pYps1-venus(LEU)	pYPS1-YFP dose response strains (low expression level)	Figure 4I	pSYC332
ySYC6-4	ySYC4-34	w303a nhp6a::nhp6a-iRFP(KAN) crz1::sfGFP-CandHIS leu::pYps1-venus(LEU)	pYPS1-YFP dose response strains (Crz1 KO)	Figure 4I	pSYC332
ySYC6-28	ySYC6-7	w303a nhp6a::nhp6a-iRFP(KAN) crz1::sfGFP-CandHIS ura::pTef1-zdk-CRZ(ALA)-mCherry-yeLANS; pTDH3-Hs_RGS2(33-67)_13aa-iRFP713 (iRFP)-asLOV2(404-546) (URA) leu::pCmk2-venus(LEU)	pCMK2-YFP dose response strains (high expression level)	Figure 4J	pSYC395
ySYC6-29	ySYC6-6	w303a nhp6a::nhp6a-iRFP(KAN) crz1::sfGFP-CandHIS ura::pRpl18b-zdk-CRZ(ALA)-mCherry-yeLANS(URA); pTDH3-Hs_RGS2(33-67)_13aa-iRFP713 (iRFP)-asLOV2(404-546)leu::pCmk2-venus(LEU)	pCMK2-YFP dose response strains (Crz1 KO)	Figure 4J	pSYC395
ySYC5-80	ySYC4-34	w303a nhp6a::nhp6a-iRFP(KAN) crz1::sfGFP-CandHIS leu::pCmk2-venus(LEU)	pCMK2-YFP dose response strains (low expression level)	Figure 4J	pSYC395
ySYC5-12	ySYC4-34	w303a nhp6a::nhp6a-iRFP(KAN) crz1::sfGFP-CandHIS ura::pADH1-CRZ(WT)-mCherry-yeLANS(URA)	Crz1 KO, Crz1-yeLANS; used for RNAseq	Supp Figure 4C	
ySYC6-33	ySYC5-36	w303a nhp6a::nhp6a-iRFP(KAN) crz1::sfGFP-CandHIS ura::pADH1-zdk-CRZ1(ALA)-mCherry-yeLANS;pTDH3-Hs_RGS2(33-67)_13aa-iRFP713 (iRFP)-asLOV2(404-546)(URA) leu::pYps1-Venus(LEU) pYPS1::TRP	Crz1*-CLASP, pYPS1-YFP promoter fusion, pYPS1 KO; used for ChIP-qPCR	Figure 6H	
ySYC6-34	ySYC5-37	w303a nhp6a::nhp6a-iRFP(KAN) crz1::sfGFP-CandHIS ura::pADH1-zdk-CRZ1(ALA)-mCherry-yeLANS;pTDH3-Hs_RGS2(33-67)_13aa-iRFP713 (iRFP)-asLOV2(404-546)(URA) leu::pGyp7-Venus(LEU) pGYP7::TRP	Crz1*-CLASP, pGYP7-YFP promoter fusion, pGYP7 KO; used for ChIP-qPCR	Figure 6H	
ySYC6-3	ySYC4-34	w303a nhp6a::nhp6a-iRFP(KAN) crz1::sfGFP-CandHIS leu::pPun1-venus(LEU)	Pun1 promoter fusion, CrzKO	background strain	pSYC331
yBMH34		w303a Nhp6a-iRFP(Kan)		background strain	
yBMH35		w303a TPK1/2/3-AS Nhp6a-iRFP (Kan)		background strain	
ySYC4-34	yBMH34	W303a Nhp6a-iRFP(Kan) crz1::HIS(candida)		background strain	
ySYC5-11	ySYC4-34	w303a nhp6a::nhp6a-iRFP(KAN) crz1::sfGFP-CandHIS ura::pADH1-CRZ(WT)-mCherry(URA)		Supp Figure 4A, 4C; background strain	pSYC295
ySYC5-13	ySYC4-34	w303a nhp6a::nhp6a-iRFP(KAN) crz1::sfGFP-CandHIS ura::pADH1-CRZ1(ALA)-mCherry(URA)		background strain	pSYC293
ySYC5-24	ySYC4-34	w303a nhp6a::nhp6a-iRFP(KAN) crz1::sfGFP-CandHIS ura::pADH1-zdk-CRZ1(WT)-mCherry-yeLANS;pTDH3-Hs_RGS2(33-67)_13aa-iRFP713 (iRFP)-asLOV2(404-546)(URA)		background strain	pSYC310
ySYC5-26	ySYC4-34	w303a nhp6a::nhp6a-iRFP(KAN) crz1::sfGFP-CandHIS ura::pADH1-zdk-CRZ1(ALA)-mCherry-yeLANS;pTDH3-Hs_RGS2(33-67)_13aa-iRFP713 (iRFP)-asLOV2(404-546)(URA)		background strain	pSYC308
ySYC5-69	ySYC4-34	w303a nhp6a::nhp6a-iRFP(KAN) crz1::sfGFP-CandHIS ura::pADH1-zdk-CRZ1(5A)-mCherry-yeLANS;pTDH3-Hs_RGS2(33-67)_13aa-iRFP713 (iRFP)-asLOV2(404-546)(URA)	precursor strain for Crz1(5A); pPun1	background strain	pSYC346
ySYC6-6	ySYC4-34	w303a nhp6a::nhp6a-iRFP(KAN) crz1::sfGFP-CandHIS ura::pRpl18b-zdk-CRZ(ALA)-mCherry-yeLANS; pTDH3-Hs_RGS2(33-67)_13aa-iRFP713 (iRFP)-asLOV2(404-546) (URA)		background strain	pSYC411
ySYC6-7	ySYC4-34	w303a nhp6a::nhp6a-iRFP(KAN) crz1::sfGFP-CandHIS ura::pTef1-zdk-CRZ(ALA)-mCherry-yeLANS; pTDH3-Hs_RGS2(33-67)_13aa-iRFP713 (iRFP)-asLOV2(404-546)(URA)		background strain	pSYC410

Table S3

Name	Background (non-GG A	Marker	Description	Notes	Addgene ID
pLO405		URA3	URA3 5' Homology-ConS-pRPL18B-Zdk1-mScarlet-yeLANS-tADH1-Con1-pRPL18B-Hs_RGS2(33-67)_13aa-iRFP713 (iRFP)-asLOV2(404-546)-tPGK1-ConE-URA3 (pSc-native-tSc)-URA3 3' Homology-KanR-ColE1	mScarlet-CLASP strain used in Figure 1 and Supplementary Figures; medium expression of mScarlet and pm-LOVTRAP	133086
pLO278		URA3	URA3 5' Homology-ConS-pRPL18B-Zdk1-VP16-ZF43_8-mScarlet-yeLANS-tADH1-Con1-pRPL18B-Hs_RGS2(33-67)_13aa-iRFP713 (iRFP)-asLOV2(404-546)-tPGK1-ConE-URA3 (pSc-native-tSc)-URA3 3' Homology-KanR-ColE1	SynTF-CLASP strain used in Figure 2 and Supplementary Figures; medium expression of SynTF and high expression of pm-LOVTRAP	
pLO388		LEU2	LEU2 5' Homology-ConLS'-pPHO84-Venus-tPGK1-ConRE'-LEU2 (pSc-native-tSc)-LEU2 3' Homology-KanR-ColE1	pPHO84 reporter	
pLO361		URA3	URA3 5' Homology-ConS-pRPL18B-Zdk1-Msn2-mScarlet-yeLANS-tADH1-Con1-pTDH3-Hs_RGS2(33-67)_13aa-iRFP713 (iRFP)-asLOV2(404-546)-tPGK1-ConE'-URA3 (pSc-native-tSc)-URA3 3' Homology-KanR-ColE1	Msn2-CLASP plasmid for strain used in Figure 2 and Supplementary Figures; medium expression of Msn2 and high expression of pm-LOVTRAP	
pLO485		URA3	URA3 5' Homology-ConLS'-pTDH3-TOM20_TMD(1-39)-iRFP713 (iRFP)-asLOV2(404-546)-tPGK1-ConRE'-URA3 (pSc-native-tSc)-URA3 3' Homology-KanR-ColE1	High expression Mito-LOVTRAP	
pLO486		URA3	URA3 5' Homology-ConLS'-pRPL18B-TOM20_TMD(1-39)-iRFP713 (iRFP)-asLOV2(404-546)-tPGK1-ConRE'-URA3 (pSc-native-tSc)-URA3 3' Homology-KanR-ColE1	Medium expression Mito-LOVTRAP	
pLO487		URA3	URA3 5' Homology-ConLS'-pREV1-TOM20_TMD(1-39)-iRFP713 (iRFP)-asLOV2(404-546)-tPGK1-ConRE'-URA3 (pSc-native-tSc)-URA3 3' Homology-KanR-ColE1	Low expression Mito-LOVTRAP	
pLO488		URA3	URA3 5' Homology-ConLS'-pTDH3-Hs_RGS2(33-67)_13aa-iRFP713 (iRFP)-asLOV2(404-546)-tPGK1-ConRE'-URA3 (pSc-native-tSc)-URA3 3' Homology-KanR-ColE1	High expression PM-LOVTRAP	
pLO489		URA3	URA3 5' Homology-ConLS'-pRPL18B-Hs_RGS2(33-67)_13aa-iRFP713 (iRFP)-asLOV2(404-546)-tPGK1-ConRE'-URA3 (pSc-native-tSc)-URA3 3' Homology-KanR-ColE1	Medium expression PM-LOVTRAP	
pLO490		URA3	URA3 5' Homology-ConLS'-pREV1-Hs_RGS2(33-67)_13aa-iRFP713 (iRFP)-asLOV2(404-546)-tPGK1-ConRE'-URA3 (pSc-native-tSc)-URA3 3' Homology-KanR-ColE1	Low expression PM-LOVTRAP	
pLO402		URA3	URA3 5' Homology-ConS-pTDH3-Zdk1-mScarlet-yeLANS-tADH1-Con1-pTDH3-Hs_RGS2(33-67)_13aa-iRFP713 (iRFP)-asLOV2(404-546)-tPGK1-ConE-URA3 (pSc-native-tSc)-URA3 3' Homology-KanR-ColE1	mScarlet-CLASP plasmid for strain used in Supplementary Figures; high expression of mScarlet and PM-LOVTRAP	
pLO407		URA3	URA3 5' Homology-ConS-pREV1-Zdk1-mScarlet-yeLANS-tADH1-Con1-pREV1-Hs_RGS2(33-67)_13aa-iRFP713 (iRFP)-asLOV2(404-546)-tPGK1-ConE-URA3 (pSc-native-tSc)-URA3 3' Homology-KanR-ColE1	mScarlet-CLASP plasmid for strain used in Supplementary Figures; low expression of mScarlet and PM-LOVTRAP	
pLO414		URA3	URA3 5' Homology-ConS-pTDH3-Zdk1-mScarlet-yeLANS-tADH1-Con1-pTDH3-TOM20_TMD(1-39)-iRFP713 (iRFP)-asLOV2(404-546)-tPGK1-ConE-URA3 (pSc-native-tSc)-URA3 3' Homology-KanR-ColE1	Zdk1-mScarlet-yeLANS + mito-LOVTRAP plasmid for strain used in Supplementary Figures; high expression of mScarlet and mito-LOVTRAP	
pLO417		URA3	URA3 5' Homology-ConS-pRPL18B-Zdk1-mScarlet-yeLANS-tADH1-Con1-pRPL18B-TOM20_TMD(1-39)-iRFP713 (iRFP)-asLOV2(404-546)-tPGK1-ConE-URA3 (pSc-native-tSc)-URA3 3' Homology-KanR-ColE1	Zdk1-mScarlet-yeLANS + mito-LOVTRAP plasmid for strain used in Supplementary Figures; medium expression of mScarlet and mito-LOVTRAP	
pLO419		URA3	URA3 5' Homology-ConS-pREV1-Zdk1-mScarlet-yeLANS-tADH1-Con1-pREV1-TOM20_TMD(1-39)-iRFP713 (iRFP)-asLOV2(404-546)-tPGK1-ConE-URA3 (pSc-native-tSc)-URA3 3' Homology-KanR-ColE1	Zdk1-mScarlet-yeLANS + mito-LOVTRAP plasmid for strain used in Supplementary Figures; low expression of mScarlet and mito-LOVTRAP	
pLO316		URA3	URA3 5' Homology-ConS-pRPL18B-VP16-ZF43_8-mScarlet-yeLANS-tADH1-Con1-pRPL18B-Hs_RGS2(33-67)_13aa-iRFP713 (iRFP)-asLOV2(404-546)-tPGK1-ConE-URA3 (pSc-native-tSc)-URA3 3' Homology-KanR-ColE1	SynTF-yeLANS plasmid for strain used in Supplementary Figures; medium expression of SynTF and PM-LOVTRAP (expressed as control for CLASP strains)	
pLO366		URA3	URA3 5' Homology-ConS-pRPL18B-Msn2-mScarlet-yeLANS-tADH1-Con1-pTDH3-Hs_RGS2(33-67)_13aa-iRFP713 (iRFP)-asLOV2(404-546)-tPGK1-ConE'-URA3 (pSc-native-tSc)-URA3 3' Homology-KanR-ColE1	Msn2-yeLANS plasmid for strain used in Supplementary Figures; medium expression of Msn2 and high expression of PM-LOVTRAP (expressed as control for CLASP strains)	
pLO344		URA3	URA3 5' Homology-ConS-pRPL18B-VP16-ZF43_8-mScarlet-NLS11-tADH1-Con1-pRPL18B-Hs_RGS2(33-67)_13aa-iRFP713 (iRFP)-asLOV2(404-546)-tPGK1-ConE-URA3 (pSc-native-tSc)-URA3 3' Homology-KanR-ColE1	SynTF-NLS plasmid for strain used in Supplementary Figures; medium expression of SynTF and PM-LOVTRAP (expressed as control for CLASP strains)	
pLO411		URA3	URA3 5' Homology-ConS-pRPL18B-VP16-ZF43_8-mScarlet-tADH1-Con1-pRPL18B-Hs_RGS2(33-67)_13aa-iRFP713 (iRFP)-asLOV2(404-546)-tPGK1-ConE-URA3 (pSc-native-tSc)-URA3 3' Homology-KanR-ColE1	SynTF-mScarlet plasmid for strain used in Supplementary Figures; medium expression of SynTF and PM-LOVTRAP (expressed as control for CLASP strains)	
pLO412		URA3	URA3 5' Homology-ConS-pRPL18B-Pho4-mScarlet-tADH1-Con1-pTDH3-Hs_RGS2(33-67)_13aa-iRFP713 (iRFP)-asLOV2(404-546)-tPGK1-ConE-URA3 (pSc-native-tSc)-URA3 3' Homology-KanR-ColE1	Pho4-mScarlet plasmid for strain used in Supplementary Figures; medium expression of Pho4 and high expression of PM-LOVTRAP (expressed as control for CLASP strains)	
pLO465		URA3	URA3 5' Homology-ConS-pRPL18B-Pho4-mScarlet-NLS11-tADH1-Con1-pTDH3-Hs_RGS2(33-67)_13aa-iRFP713 (iRFP)-asLOV2(404-546)-tPGK1-ConE-URA3 (pSc-native-tSc)-URA3 3' Homology-KanR-ColE1	Pho4-NLS plasmid for strain used in Supplementary Figures; medium expression of Pho4 and high expression of PM-LOVTRAP (expressed as control for CLASP strains)	
pLO463		URA3	URA3 5' Homology-ConS-pRPL18B-Msn2-mScarlet-NLS11-tADH1-Con1-pTDH3-Hs_RGS2(33-67)_13aa-iRFP713 (iRFP)-asLOV2(404-546)-tPGK1-ConE'-URA3 (pSc-native-tSc)-URA3 3' Homology-KanR-ColE1	Msn2-NLS plasmid for strain used in Supplementary Figures; medium expression of Msn2 and high expression of PM-LOVTRAP (expressed as control for CLASP strains)	
pLO480		URA3	URA3 5' Homology-ConS-pRPL18B-Msn2-mScarlet-tADH1-Con1-pTDH3-Hs_RGS2(33-67)_13aa-iRFP713 (iRFP)-asLOV2(404-546)-tPGK1-ConE'-URA3 (pSc-native-tSc)-URA3 3' Homology-KanR-ColE1	Msn2-mScarlet plasmid for strain used in Supplementary Figures; medium expression of Msn2 and high expression of PM-LOVTRAP (expressed as control for CLASP strains)	
pLO364		URA3	URA3 5' Homology-ConS-pRPL18B-Zdk1-Gal4-mScarlet-yeLANS-tADH1-Con1-pTDH3-Hs_RGS2(33-67)_13aa-iRFP713 (iRFP)-asLOV2(404-546)-tPGK1-ConE-URA3 (pSc-native-tSc)-URA3 3' Homology-KanR-ColE1	Gal4-CLASP plasmid for strain used in Supplementary Figures; medium expression of Gal4 and high expression of PM-LOVTRAP	
pLO413		URA3	URA3 5' Homology-ConS-pRPL18B-Zdk1-Gal4-mScarlet-tADH1-Con1-pTDH3-Hs_RGS2(33-67)_13aa-iRFP713 (iRFP)-asLOV2(404-546)-tPGK1-ConE-URA3 (pSc-native-tSc)-URA3 3' Homology-KanR-ColE1	Gal4-mScarlet plasmid for strain used in Supplementary Figures; medium expression of Gal4 and high expression of PM-LOVTRAP (expressed as control for CLASP strain)	
pAN736		LEU2	LEU2 5' Homology-p43_8(8x)-Venus-tPGK1-LEU2 (pSc-native-tSc)-LEU2 3' Homology-KanR-ColE1	pSynTF reporter	

Table S3

pLO363		URA3	URA3 5' Homology-ConS-pRPL18B-Zdk1-Pho4-mScarlet-yeLANS-tADH1-Con1-pTDH3-Hs_RGS2(33-67)_13aa-iRFP713 (iRFP)-asLOV2(404-546)-tPGK1-ConE-URA3 (pSc-native-tSc)-URA3 3' Homology-KanR-ColE1	Pho4-CLASP plasmid for strain used in Figure 2 and Supplementary Figures; medium expression of Pho4 and high expression of PM-LOVTRAP	
pLO352		LEU2	LEU2 5' Homology-ConS-pHsp12-Venus-tPGK1-ConE'-LEU2 (pSc-native-tSc)-LEU2 3' Homology-KanR-ColE1	pHSP12 reporter	
YTK120		HIS3	C.G. HIS3	HIS3 cassette	
pAN160		LEU2	LEU2 5' Homology-ConS-pGal1-Venus-tPGK1-ConE-LEU2 (pSc-native-tSc)-LEU2 3' Homology-KanR-ColE1	pGAL1 reporter	
pSYC084	pSYC081	TRP1	pAdh1-mCherry-PEF-NESLOVNLS-JSO179	original LANS Yumerefendi 2015	
pSYC085	pSYC084	TRP1	pAdh1-mCherry-PEF-NESLOVNLSvar#3-JSO179	NLS variant	
pSYC086	pSYC084	TRP1	pAdh1-mCherry-PEF-NESLOVNLSvar#4-JSO179	NLS variant	
pSYC087	pSYC084	TRP1	pAdh1-mCherry-PEF-NESLOVNLSvar#5-JSO179	NLS variant	
pSYC088	pSYC084	TRP1	pAdh1-mCherry-PEF-NESLOVNLSvar#8-JSO179	NLS variant	
pSYC089	pSYC084	TRP1	pAdh1-mCherry-PEF-NESLOVNLSvar#9-JSO179	NLS variant	
pSYC090	pSYC084	TRP1	pAdh1-mCherry-PEF-NESLOVNLSvar#11-JSO179	NLS variant (yeLANS)	
pSYC091	pSYC084	TRP1	pAdh1-mCherry-PEF-NESLOVNLSvar#14-JSO179	NLS variant	
pSYC092	pSYC084	TRP1	pAdh1-mCherry-PEF-NESLOVNLSvar#15-JSO179	NLS variant	
pSYC093	pSYC084	TRP1	pAdh1-mCherry-PEF-NESLOVNLSvar#20-JSO179	NLS variant	
pSYC094	pSYC084	TRP1	pAdh1-mCherry-PEF-NESLOVNLSvar#24-JSO179	NLS variant	
pSYC095	pSYC084	TRP1	pAdh1-mCherry-PEF-NESLOVNLSvar#27-JSO179	NLS variant	
pSYC096	pSYC084	TRP1	pAdh1-mCherry-PEF-NESLOVNLSvar#29-JSO179	NLS variant	
pSYC081	pJSO179	TRP1	PEF_NESLOVNLS_SacI-JSO179	intermediate plasmid	
pJSO179	pNH604	TRP1	p604; basic single integration vector from Lim lab	base plasmid	
pJSO529	pNH604	TRP1	604-Adh1-Dot6-mCherry	tagged TF to test for localization dynamics in response to environmental inputs	
pJSO568	pNH604	TRP1	604-pAdh1-Crz1-mcherry	tagged TF to test for localization dynamics in response to environmental inputs	
pJSO269	pNH604	TRP1	604-pAdh1-Stb3-mCherry	tagged TF to test for localization dynamics in response to environmental inputs	
pJSO392	pNH604	TRP1	604-pAdh1-MSN2-mCherry	tagged TF to test for localization dynamics in response to environmental inputs	
pJSO285	pNH604	TRP1	604-pAdh1-Msn4-mCherry	tagged TF to test for localization dynamics in response to environmental inputs	
pJSO569	pNH604	TRP1	604-pAdh1-Pho4-mcherry	tagged TF to test for localization dynamics in response to environmental inputs	
pSYC332		LEU2	pYPS1-Venus	promoter fusion	133118
pSYC392		LEU2	pGYP7-Venus	promoter fusion	133120
pSYC393		LEU2	pPUT1-Venus	promoter fusion	
pSYC395		LEU2	pCMK2-Venus	promoter fusion	133119
pSYC398		LEU2	pENA1-Venus	promoter fusion	
pSYC400		LEU2	pMEP1-Venus	promoter fusion	
pSYC331		LEU2	pPUN1-Venus	promoter fusion	
pSYC295		URA3	pADH1-Crz1-mcherry-tPGK1	Crz1 WT characterization	
pSYC293		URA3	pADH1-Crz1(19A)-mcherry-tPGK1	Crz1* characterization	
pSYC310		URA3	pADH1-zdk-Crz1-mcherry-yeLANS-tPGK1; pTDH3-Rgs2-iRFP713-asLOV2(404-546)-tPGK1	Crz1 WT - CLASP characterization	
pSYC308		URA3	pADH1-zdk-Crz1(19A)-mcherry-yeLANS-tPGK1; pTDH3-Rgs2-iRFP713-asLOV2(404-546)-tPGK1	Crz1*-CLASP characterization	133085
pSYC346		URA3	pADH1-zdk-Crz1(5A)-mcherry-yeLANS; pTDH3-Rgs2-iRFP713-asLOV2(404-546)-tPGK1	Crz1 5A - CLASP characterization	
pSYC410		URA3	pTEF1-zdk-Crz1(19A)-mcherry-yeLANS; pTDH3-Rgs2-iRFP713-asLOV2(404-546)-tPGK1	Crz1*-CLASP dose response	
pSYC411		URA3	pRPL18b-zdk-Crz1(19A)-mcherry-yeLANS; pTDH3-Rgs2-iRFP713-asLOV2(404-546)-tPGK1	Crz1*-CLASP dose response	

Table S4

Light Dose	milliWattage	Std Dev	Date
0	-0.0001499	0.0002004	20181205
0	-0.0002513	0.000252	20181128
0	-0.001819	0.000978	20181109
64	0.1011	0.008522	20181205
64	0.07921	0.007053	20181128
64	0.1279	0.01123	20181109
128	0.1944	0.02126	20181205
128	0.1962	0.01824	20181128
128	0.2633	0.02653	20181109
256	0.3961	0.0393	20181205
256	0.4012	0.0362	20181128
256	0.5107	0.04832	20181109
512	0.7849	0.07396	20181205
512	0.7776	0.09084	20181128
512	1.041	0.09508	20181109
1024	1.53	0.1346	20181205
1024	1.477	0.1491	20181128
1024	1.986	0.2349	20181109
2048	3.088	0.3326	20181205
2048	3.026	0.2563	20181128
2048	3.45	0.9	20181109
3072	4.302	0.4414	20181205
3072	4.235	0.4559	20181128
4095	5.407	0.5494	20181205
4095	5.486	0.4617	20181128
4095	6.56	0.587	20181109